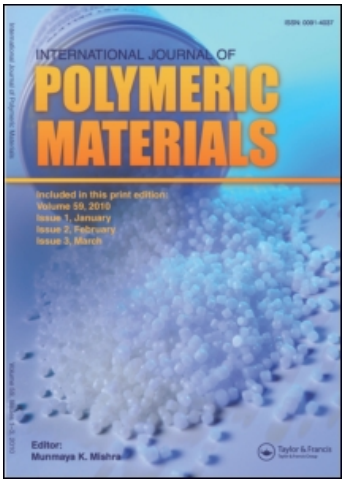

International Journal of Polymeric Materials
Publication details, including instructions for authors and subscription information:
http://www.informaworld.com/smpp/title~content=t713647664

Solvation Properties of Biopolymers

A. J. Hopfinger[a]
[a] Department of Macromolecular Science, Case Western Reserve University Cleveland, Ohio, U.S.A.

To cite this Article Hopfinger, A. J.(1975) 'Solvation Properties of Biopolymers', International Journal of Polymeric Materials, 4: 1, 79 — 159
To link to this Article: DOI: 10.1080/00914037508072349
URL: http://dx.doi.org/10.1080/00914037508072349

Solvation Properties of Biopolymers

A. J. HOPFINGER

Department of Macromolecular Science, Case Western Reserve University Cleveland, Ohio 44106, U.S.A.

This paper reviews work carried out in the elucidation of the solvation properties of biopolymer solutions. Studies dealing with the molecular aspects of biopolymer-solution organization are emphasized. Classic theories of polymer solutions are presented in the Introduction to lay a background for the more current studies discussed in the following sections of the report. The second part of the paper discusses several experimental studies dealing with the interrelationship between biopolymer chain conformation and solvent ordering about the biopolymer. Applications of IR, NMR and thermocalorimetric techniques to solution studies are presented. The third section of the manuscript covers current molecular theories being used to characterize the molecular thermodynamics of polymer-solvent interactions. Extensive discussion of the hydration-shell model, and its application to biopolymer solutions, is presented. The next section deals with protein denaturation and the role which protein-solvent interactions play in governing the behavior of this process. The last section of the manuscript presents the highlights of several investigations which are not directly concerned with, but are related to, the organization of solute and solvent structures in biopolymer solutions. In presenting these studies the applications of ORD/CD, ultraviolet, NMR, X-ray diffraction, electric birefringence and IR spectroscopies in solution studies are considered.

1 INTRODUCTION

The purpose of this paper is to review our understanding of what happens when a solute macromolecule is placed in a solvent medium. At the outset let us stipulate that the macromolecule is much larger than the solvent molecule(s). This restriction generates a special case of the general phenomenon of the behavior of two or more components which are allowed to interact such that at least one of the components serves as a fluid medium for the other

---

†Presented at the Midland Macromolecular Meeting on "Order in Polymer Solutions", August 20–24, 1973.

component(s). This general process is termed *solvation* and we, in this paper, will discuss the solvated state of macromolecules.

Perhaps the most notable breakthrough in the development of a theory of polymer solutions was made nearly simultaneously, but independently, by Flory[1] and Huggins.[2] They reasoned that the entropy of a polymer solution must be small in comparison to a solution of non-polymer liquids based upon the same volume, or weight, concentrations because both the size and the connectivity of the polymer chain keep the chain-entropy small in comparison to that of a non-polymeric species. Flory and Huggins, again independently, were able to derive approximate expressions for the number of configurational states a polymer chain could adopt in solution using a lattice model. This laid the basis for what is now called the Flory-Huggins theory of polymer solutions. This theory introduced a most basic parameter, χ_1,† which in the Flory-Huggins theory characterizes the total interaction energy of the solution per solvent molecule divided by kT times the volume fraction of the polymer.

The first polymer solution for which experimental results were compared with the Flory-Huggins theory was that of rubber in benzene.[3] Outside of fair agreement between theory and experiment for the free energy of mixing the theory was not particularly successful. Discrepancies between theory and experiment grew larger with increasing dilution. Additional experiments on different systems supported the supposition that the Flory-Huggins theory could only be successful for reasonably concentrated polymer solutions, and was not at all adequate for dilute systems.

The reason for this is that the lattice model used in the Flory-Huggins model does not consider that a very dilute polymer solution must be discontinuous in structure, consisting of domains or clusters of polymer chains separated, on the average, by regions of bulk solvent. Flory and Krigbaum[4] modelled such a discontinuous structure. They assumed a model in which each cloud of polymer chain segments is spherical, with a density that is maximum at the center of the sphere and decreases in a Gaussian fashion with distance from the center. The Flory-Krigbaum theory, as this model has come to be known, is reasonably successful in describing some dilute polymer solutions. Just as with the Flory-Huggins theory, one is never quite sure when the Flory-Krigbaum theory can be validly applied.

Furthermore, both the Flory-Huggins and Flory-Krigbaum theories assume that polymeric solutions differ from monomeric solutions only through the contributions to the entropic term. Detailed studies of the deviations between theory and experiment for the interaction parameter χ_1 have led to its re-interpretation as a combined entropy and enthalpy parameter. The major

---

†Huggins adopted μ_h° instead of χ_1.

contribution to the χ_1-parameter for polymer-solvent systems arises through the differences in free volumes.

Recognition of a volume-dependent enthalpy contribution in the characterization of a polymer solution has led to the development of several elegant "free-volume" theories of polymer solutions. The pioneering work in this area was carried out by Prigogine and his co-workers,[5] with the development of "corresponding states theory" and extended and put into practice by Flory[6-10] as well as by Patterson.[11-12] These theories recognize the dissimilarity in the free volumes of the polymer and the solvent as a result of their great difference in size, the usual solvent being more expanded than the polymer. These free volume theories are usually more accurate than the prior polymer-solution theories in that volume changes on mixing can be predicted to within 10–15% of the experimental values and the correct variation of χ_1 in the Flory-Huggins theory, with concentration is also predicted.

In 1959 Maron[13] introduced a semi-empirical theory of polymer solutions based upon the *effective* volume of the solute molecule in the solvent medium. In this theory a characteristic interaction parameter μ, which takes into account both enthalpy and entropy contributions from solvent-solvent, solvent-solute and solute-solute interactions, takes the place of χ. Because μ is determined from all three types of interactions in a two-component solution the Maron theory is applicable over a wide range of concentrations and for a large number of solution-types. It is *not* restricted to only polymer solutions. References 14 and 15 contain composite listings of solutions to which Maron theory has been applied. Although not used, or known, extensively this may be one of the better polymer-solution theories presently available.

What we would now like to do is to dissect, on the molecular level, the interaction parameter, μ, which, as mentioned earlier, tells us how polymer-polymer, polymer-solvent, and solvent-solvent interactions modify the properties of a polymer solution from those of "regular solutions". Most of the discussion will focus upon polymer-solvent interactions, but a limited discussion of the other two types of interactions will also be presented. Furthermore, the studies reported here will deal with biopolymers, especially polypeptides in an aqueous medium. This really should not be too surprising since the majority, or at least the largest minority, of solution studies carried out in the last fifteen years have been by protein chemists and biophysicists.

Many of the studies presented here deal with the interrelationship between the interactions which take place in a polymer solution and the corresponding spatial organization of the polymer chains in solution. These studies introduce a new dimension to the elucidation of the nature of polymer solutions. The reader will recall that the polymer-solution theories discussed earlier in this section *assume* a particular molecular geometry. The predicted thermodynamic quantities are a consequence of the assumed geometry. In several of

the theoretical molecular studies to be discussed, the molecular geometry, i.e. chain conformation(s), is a *predicted consequence* of the molecular energetics of solvent molecules interacting with polymer chains. Hence, these molecular studies, in a sense, evaluate the reasonableness of some of the geometries assumed in the early theories. Moreover, the studies which relate polymer-solvent interactions to polymer-chain conformation represent a head-on attack to one of the fundamental questions in polymer chemistry; namely, the molecular behavior of macromolecules in the solvated state.

2 EXPERIMENTAL STUDIES OF ORDERING IN BIOPOLYMER SOLUTIONS

The problem of protein hydration has been given a great deal of attention over the last four decades.[16-20] Early workers[16] in the field held the view that the bulk of the hydration water is bound to the polar groups (*e.g.*, carboxylic, amino) of the proteins, and that the binding processes responsible are governed, in the main, by the laws of chemical equilibria. This idea was supported by work on fibrous proteins such as keratin. For example, Watt and Leeder[21] were able to account for the uptake of water in wool fibers by postulating the existence of chemical equilibria. Unfortunately it was not possible to access the role of chain conformation and changes in chain conformation on the conditions of chemical equilibria in natural systems.

The heterogenity of the polypeptide chains coupled with the complexity of the tertiary and ultra-structures make controlled structure-solvent studies extremely difficult on natural biopolymers. This fact was recognized by Breuer and Kennerley[22] who determined water binding isotherms of a series of homopolypeptide films. A typical set of water-binding isotherms is shown in Figure 1 which demonstrates the effect of peptide sidechain upon water-binding. Homopolypeptides containing polar sidechains, such as poly(L-lysine), bind more water than homopolypeptides with nonpolar sidechains, such as polyglycine. Using a binding isotherm like those shown in Figure 1 it is possible to determine the number of adsorption sites, n, per amino acid residue. Table 1 contains the values of n for some homopolypeptides. Obviously this idea of a "all or none" interaction as implied by the concept of an adsorption site is an oversimplification of the dynamic process of polymer and solvent interacting. However, it does provide a frank conceptual understanding of the problem. From these measurements Breuer and Kennerley concluded that water uptake is proportional to the thickness of the film which, in turn, suggests that the binding sites are not confined to the surface of the film but are distributed throughout the film.

Chirgadze and Ovsepyan[23] have recently reviewed the work done on the

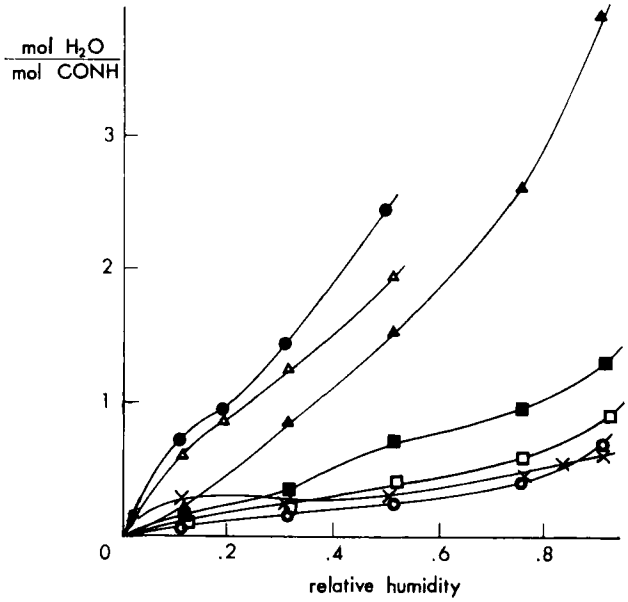

FIGURE 1 Water-binding isotherms for some polypeptides. (○) Poly(L-alanine), (□) polyglycine I, (×) polyglycine II, (■) poly(L-glutamic acid), (▲) poly(L-lysine), (△) poly-(L-lysine·HBr), (●) sodium salt of poly(L-glutamic acid). Reprinted from Ref. (22) by courtesy of Academic Press, Inc.

TABLE I

Number of water binding sites of the various polypeptide residues[a]

	n
Poly(glycine)	1
Poly(alanine)	1
Poly(glutamic acid)	2
Poly(lysine)	4
Poly(Na glutamate)	3
Poly(lysine·HBr)	4

[a]From Ref. (22) by courtesy of Academic Press, Inc.

influence of water vapor pressure on the structure of the hydrochlorides of poly(L-lysine), poly(L-glutamic acid) and its sodium salt. These systems were investigated by Blout and Lenormant,[24] Shmueli and Traub[25] and Kobyakov.[26] These authors showed that in films these polypeptides undergo conformational changes which depend upon the humidity. Infrared spectroscopy[24,26] and

X-ray analysis[25] were used to monitor structural changes. On the basis of data from the above mentioned papers Chirgadze and Ovsepyan were able to construct the quasi "phase diagram" shown in Figure 2 for poly(L-lysine hydrochloride).

In a film prepared from an aqueous solution at room temperature and relative humidity of about 50%, a part of the sample has the helical structure; it is denoted as α'. (In the infrared spectrum the amide I band has a frequency of 1655 cm^{-1}.) The other part of the sample is in the β form, the main component of the amide I being 1625 cm^{-1}. The sample transforms completely into the β form if it is exposed for several hours to a humidity of 65%. At this humidity the number of water molecules per peptide residue is approximately 2. An increase of the humidity from 65% to 100% causes no changes. An exposure at a humidity of 100%, for short periods of time, leads to a transition of the extended form into the helical, but of a somewhat different type, α'' (amide I 1645 cm^{-1}). The $\beta \rightarrow \alpha''$ transition is reversible. In the α'' form, the number of water molecules per residue is 4–6; however, in an aqueous solution the polymer has a random form. The transition from the helical to the random state occurs when fifteen water molecules are bound to a residue.[25] Kobyakov has shown[26] that the α'' and the random forms can be fixed by rapid drying at low

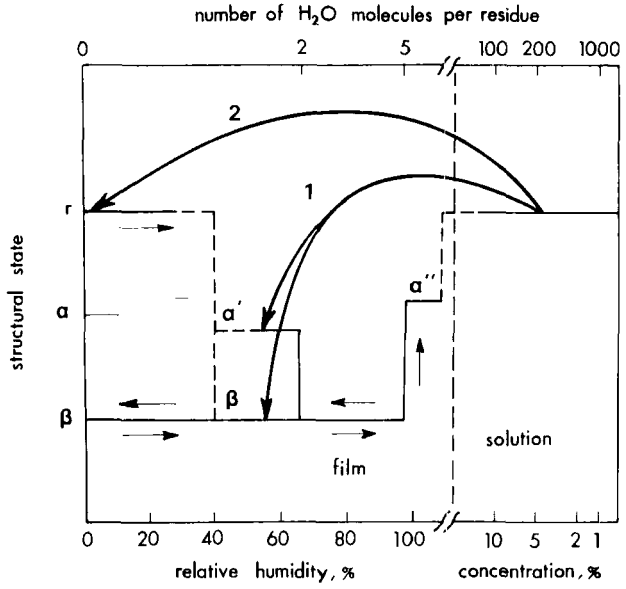

FIGURE 2 Diagram of the dependence of the state of poly(L-lysine·HCl) on the humidity, based on the data from Refs. (24, 25). α, β and r denote α-helix, β-form, and random state. The rapid transition from the solution to the solid state at the given humidity is shown by arrows 1 and 2. Reprinted from Ref. (23) by courtesy of John Wiley & Sons, Inc.

humidity; the fixed state can be preserved at higher humidities up to 40–50%. If the sample is in the β form at room temperature, the sequential dehydration to zero humidity does not lead to a change of the structure.

These facts show that the hydrochloride of poly(L-lysine) [as well as that of poly(L-glutamic acid) and its salt] changes its conformation depending on the water vapor pressure. The investigated polypeptides are models for studying many common features of peptide compounds. However, general properties of hydrational transitions for these polypeptides are somewhat distorted since these model compounds are regular polymers, in contrast to naturally occurring polypeptides. The regularity of the model compounds will also affect the polyelectrolyte behavior.

There has been an ever increasing number of studies concerning the ordering of water molecules about polypeptides using IR and near-infrared spectroscopy. The near-infrared spectroscopic method for studying protein hydration constitutes an approach whereby "bound water"† can be distinguished from bulk water since differences in bonding manifest themselves in the generation of different signals. McCabe and Fisher[27] have demonstrated that the near-infrared difference spectra of aqueous solutions measured versus water itself contain three components: (1) a negative component consisting of an absolute spectrum of the amount of water excluded by the hydrated solute; (2) a positive component contributed by the hydrated water, and (3) an additional component consisting of the absorption (if any) of the solute. By applying a correction for the "excluded volume" and solute absorption, it is possible to obtain "hydration spectra".[28] Subramanian and Fisher[29] have used this method to determine volume changes and differences in hydration that occur during a helix-coil transition of two polypeptides poly(L-glutamic acid) (PGA) and poly(L-lysine) (PLL). The transition was induced by changing the pH, and the pH difference spectra were measured maintaining equal concentrations of the polypeptide in reference and sample cells.

The pH difference spectra of PLL and PGA are shown in curves *a* and *b*, respectively, of Figure 3. Addition of a spectrum of an amount of water representing the difference in excluded volume between the helical and coiled forms of PLL to curve *a*, results in curve *c*. The pH difference spectrum for lysine · HCl and the same spectrum corrected for excluded volume are presented in Figure 4. The pH difference spectra for *n*-butylamine and aniline (corrected for excluded volume) are shown in Figure 5.

As can be seen from Figure 3, the total volume change in a helix-coil transition is small, confirming previous studies,[30,31] and could not be apportioned into volume changes due to helix-coil transition and ionization equilibria. In

†The term "bound" may be a misleading description. There are 15 water molecules per residue based upon the ratio of the two components of the system.

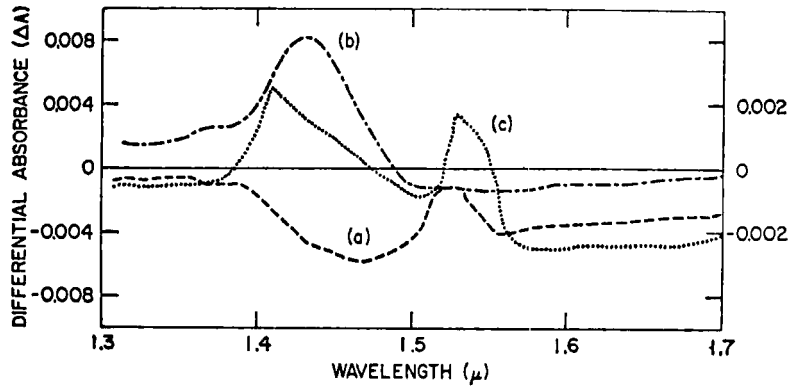

FIGURE 3 pH difference spectra of poly(L-lysine) and poly(L-glutamic acid); path length 0.1 cm, $T = 20°C$. (*a*) 0.09 *M* PLL, pH 10.8 (sample) *vs.* pH 7.8 (reference); (*b*) 0.13 *M* PGA, pH 4.4 (sample) *vs.* pH 8.0 (reference). (*c*) Resultant spectrum after addition of a water spectrum representing the excluded volume, to curve *a*. The water spectrum was added after normalizing the spectrum of water at $\approx 1.46\ \mu$ (in the region of λ_{max} for water) instead of at $1.68\ \mu$ cited in Ref. (28) since the NH_3^+ group has some residual absorption at $1.68\ \mu$. For more details see Ref. (28). Scale: left ordinate for *a* and *b*, right ordinate for *c*. Reprinted from Ref. (29) by courtesy of John Wiley & Sons, Inc.

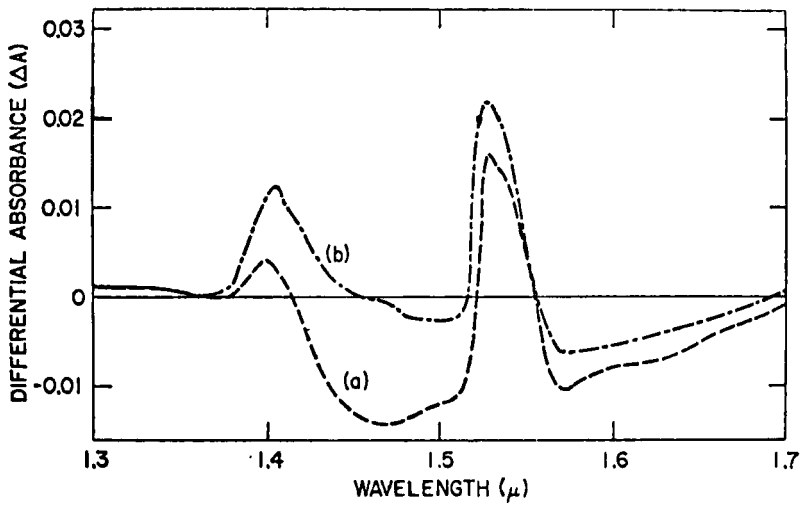

FIGURE 4 pH difference spectrum of lysine; path length 0.1 cm, $T = 20°C$. (*a*) pH 12 (sample) *vs.* pH 8.0 (reference), concentration 0.3 *M*; (*b*) water spectrum added to curve *a*. Reprinted from Ref. (29) by courtesy of John Wiley & Sons, Inc.

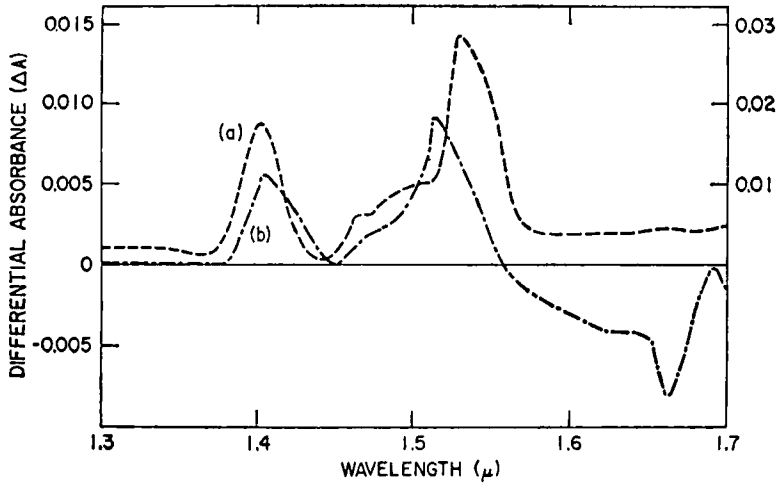

FIGURE 5 pH difference spectra of *n*-$BuNH_2$ and aniline; path length 0.1 cm, $T = 20°C$. (*a*) 0.6 *M* *n*-$BuNH_2$, pH 11.5 (sample) *vs.* pH 9.0 (reference), right ordinate scale; (*b*) 0.2 *M* aniline, pH 5.6 (sample) *vs.* pH 3.5 (reference), left ordinate scale. Reprinted from Ref. (29) by courtesy of John Wiley & Sons, Inc.

effect then, this study represents only hydration differences during a helix-coil transition.

Curve *c* in Figure 3 contains a positive peak centered at 1.527 μ (6554 cm^{-1}), another positive peak at 1.406 μ (7114 cm^{-1}) and a broad negative absorption at wavelengths greater than 1.54 μ. The positive peak at 1.527 μ should arise from the first NH stretch overtone as noted with amides and amines.[32] This peak may be due to differential absorption of peptide NH bond in the helical and coiled forms or the side-chain amino group of PLL. In the pH difference spectrum of PGA such a peak is absent, and hence the 1.527 μ peak must be due to the ε-amino group. The NH_2 group has a sharp absorption band[33] while the NH_3^+ group has a diffuse band. Therefore, the 1.527 μ band is assigned to the unionized ε-NH_2 group in the helical PLL (sample cell) and the negative absorption at wavelengths > 1.54 μ to the ionized amino group in the coiled form (reference cell).

Similar pH difference spectra (unionized versus ionized amino groups) for poly(L-lysine) side chain analogs like lysine·HCl and *n*-butylamine show positive peaks at 1.531 μ and 1.528 μ, respectively (Figures 4 and 5(a)). This observation reinforces the suggestion that the positive peak at 1.527 μ in the PLL spectrum (Figure 3(c)) must arise from the unionized ε-amino group.

In the spectra of lysine and *n*-$BuNH_2$ there is a shoulder at 1.54 μ in addition to the peak at ≈ 1.53 μ. In proton-accepting solvents such as DMSO, the NH_2 absorption of $BuNH_2$ shifts to 1.542 μ from a value of 1.525 μ in a non-proton-

accepting solvent like CCl_4. If it is assumed that the peak at 1.53 μ is due to free NH, then the shoulder at 1.54 μ in the spectra of lysine and n-$BuNH_2$ could be due to an H-bonded NH in a situation such as:

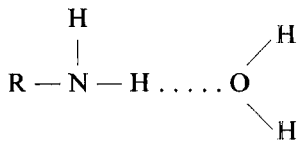

If this statement is true, then the water which is H-bonded to the amino group should have an absorption peak of its own in the difference spectrum. Such an absorption peak is noticed at 1.406 μ for PLL, at 1.408 μ for lysine, and at 1.402 μ for n-$BuNH_2$.

A pH difference spectrum of aniline (Figure 5(b)) (unionized versus ionized amino group) has features similar to those of lysine and n-$BuNH_2$. There are positive peaks at 1.403 μ and 1.516 μ and negative absorption at wavelengths > 1.56 μ. Aniline in CCl_4 has the major peak at 1.494 μ which shifts to 1.53 μ in proton-accepting solvents. On this basis, the peak at 1.516 μ for aniline in water can be attributed to the H-bonded NH_2 group while that at 1.403 μ must be due to the hydrated water, since the amino group has no absorption in the 1.4 μ region.

The peak in the 1.4 μ region is therefore due to a water molecule (a combination band, $\nu_1 + \nu_3$) H-bonded to the NH_2 group, be it in a PLL helix, lysine, $BuNH_2$, or aniline. The λ_{max} for this peak is 1.405 ± 0.003 μ in the various systems studied. Water in CCl_4 (monomeric) has a λ_{max} at 1.4 μ for the $\nu_1 + \nu_3$ band[34] and a water molecule whose lone pairs but not hydrogens are engaged in H-bonding does not differ significantly[35] in absorption properties from a water monomer. Accordingly, the 1.405 μ peak can be assigned to the hydrated water involving the lone pairs on oxygen in H-bonding to the amino group.

Differences, if any, between the peptide NH frequencies in the coil and helical forms of the polypeptides are not observable in accordance with the observation of Doty and Gratzer.[36] One would expect the CO and NH groups to be hydrated in the random coil and accordingly such hydrated water should show absorption as negative peaks in the 1.4 μ region in the difference spectra of PLL and PGA, since the CO and NH groups are more abundant than the side-chain groups. The positive instead of negative peak in the 1.4 μ region is rather surprising. Perhaps several of the CONH groups are bonded[36] to other CONH groups in the random coil and hence the peptide hydration signal is not observed.

The broad band at 1.43 μ in the pH difference spectrum of PGA is assigned to the γ-COOH in the helical form in analogy with the pH difference spectrum

of acetic acid. It seems the γ-COOH in the PGA helix interacts with water much in the same way as the carboxyl group of acetic acid does.

Buontempo, Careri and Fasella[37] used infrared spectroscopy to study the ordering of water molecules about globular proteins. They found, using lysozyme and bovine serum albumin, that the band near 3300 cm^{-1}, due to the NH stretching in the protein backbone, displays not only two distinct peaks centered around 3400 and 3260 cm^{-1} in the hydration difference spectrum, as found by Bendit[38] in his studies of keratin, but also a shoulder in the amide B region. The enhancement of the amide B band provides conclusive evidence that the NH band profile is affected by water binding. They propose that the hydration peak near 3260 cm^{-1} is due to two concurrent phenomena in addition to the red shift of the NH band first proposed by Bendit[38]: (a) enhancement by bound water of the combination peak near 3220 cm^{-1},[39] and (b) presence of a peculiar water having an IR spectrum similar to that of ice.

Engel and coworkers have reported a series of infrared studies of the interaction of different solvents with peptides.[40,41] Representative of these studies is the work carried out on cyclotri(L-prolyl) (CTP) and linear poly(*O*-acetyl hydroxyproline) (POAP).[42] The emphasis in the study was to determine the binding properties of peptide CO groups which are freely accessible to the solvent as in poly(L-proline) (PP II), but which are in *cis* configuration as in PP I. A stereo-chemical analysis of CTP has shown[43] that its peptide bonds cannot assume the *trans* configuration for steric reasons and that a *cis* configuration with a non-planarity of $\Delta\omega$[44] approximately $-25°$ is the most likely arrangement. A spatial arrangement of the peptide groups similar to that in the I helix has been suggested on the basis of circular dichroism spectra.[45] The six membered ring of cyclodi-prolyl (proline diketopiperazine) does not resemble a turn of the I helix although this compound also contains *cis*-peptide bonds. It is for this reason that CTP was preferred in their study.

The stretching vibration (amide I band) of the free peptide CO groups is observed at 1644 cm^{-1} (see Table II) when CTP is dissolved in dichloromethane which does not form hydrogen bonds. Compared with POAP I the

TABLE II

Position of the amide I band characteristic for free and bound peptide CO groups in cyclotri(L-prolyl), poly(*O*-acetyl-L-hydroxyproline) I and II

State of peptide CO groups	Wave number (cm^{-1})		
	Cyclotri(L-prolyl)	Poly(*O*-acetyl-L-hydroxyproline) I	II
Free in dichloromethane	1644	1654	1659
Bound in benzyl alcohol	1620	1647	1648

band is displaced to lower frequencies by 10 cm^{-1}. The opposite displacement is expected on the basis of the decreased planarity of the peptide group in CTP which would tend to strengthen the double-bond character of the CO groups. It must be kept in mind, however, that the position of the amide I band also depends on other effects, *e.g.*, on the coupling between CO groups in the same molecule.

As in the case of PP and POAP, a second component of the amide I band appears at decreased wave number (1630 cm^{-1}, see Table II) when alcohol is added to a solution of CTP in dichloromethane. This new band is attributed to the stretching vibration of CO groups to which alcohol is bound via hydrogen bonds.[41] The shift in wave number $\Delta\nu = 14$ cm^{-1} is somewhat larger than that observed for POAP II ($\Delta\nu = 11$ cm^{-1}) and twice as large as that for the same polymer in the helix I conformation ($\Delta\nu = 7$ cm^{-1}). This indicates that the negative enthalpies of the binding of benzyl alcohol to CTP and POAP II are comparable and larger than in the case of POAP I.

An estimate of the binding constants was obtained from the ratio of the band intensities. The area beyond the 1630 cm^{-1} band divided by the total area of the profile equals the fraction of bound CO groups f_b under certain assumptions. The band separation procedure was the same as in Ref. 41. A plot of f_b versus the molar fraction of benzyl alcohol in dichloromethane yields the binding curve (see Figure 6). A comparison of the result with binding curves obtained for the polymer in the I and II conformation shows that the binding constant K of benzyl alcohol to peptide CO groups is about the same for CTP and POAP II ($K = 20$–30), whereas it is much smaller for POAP I ($K = 5$–10).

The close similarity of the binding properties of CTP and POAP in the helix II

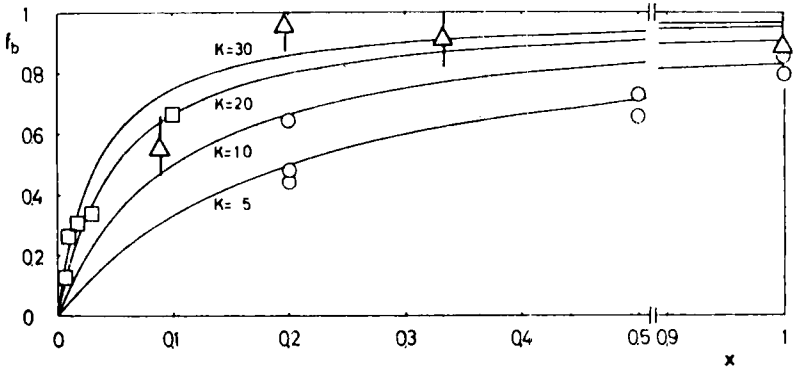

FIGURE 6 Fraction of bound peptide groups CO, f_b, of cyclotri(L-prolyl) (△), poly-(*O*-acetyl-L-hydroxyproline) in helix II conformation (□) and helix I conformation (○) *vs.* mole fraction of benzyl alcohol in dichloromethane, x. The curves are calculated for a simple binding equilibrium with a single binding constant K from $f_b = Kx/(1 + Kx)$. Reprinted from Ref. (42) by courtesy of John Wiley & Sons, Inc.

conformation indicates that (as was previously assumed[41]) special steric effects are responsible for the weaker binding of alcohols to PP and its derivatives in the helix I conformation. It may be this effect and the resulting small difference in binding strength which causes PP I to be stable in solvents which are weak hydrogen bond donors and to convert to PP II in the presence of strong hydrogen-bonding solvent partners.[41,46] In a related IR study which supports this contention, Swenson and Formanek[47] have demonstrated that water molecules are hydrogen-bonded to the carbonyl carbons of PP II, but not PP I.

Perhaps the most promising technique to study the molecular dynamics of solute-solvent interactions is NMR. Fuller and Brey[48] as well as Kuntz and coworkers[49] have used NMR to demonstrate the existence of a peculiar state of water in globular proteins, in agreement to that reported above in the IR studies of Buontempo *et al.*,[37] at high hydration coverage. These NMR experiments also show that this state of water is incapable of crystallizing under conditions where the surrounding bulk water crystallizes, and that it retains its peculiar properties at a temperature as low as −60°C. Berendsen[50] carried out one of the most elegant NMR studies when he attempted to determine the structuring of water molecules about the fibrous protein collagen. Unfortunately, the results of this study are not conclusive and still remain open to inquiry. Glasel[51] made use of the dynamic capabilities of NMR spectroscopy when he studied the polymer-solvent interactions of a variety of polymers, with various types of sidechains in D_2O. By plotting the relaxation rate, $1/T_1$, and viscosity as functions of the concentration and pH, he was able to make some deductions about the characteristic polymer-solvent interactions.

Poly(methacrylic acid), poly(L-lysine), and poly(L-glutamic acid) each undergo a conformational transition as a function of pH. This is reflected in the $1/T_1$ *vs.* pH curves presented in Figure 7. There is, for all three polymers, a definite change in the relaxation rate over a relatively small range of pH. Glasel, using data obtained from plots of the type given in Figure 7, has postulated the following phenomenological rules concerning D_2O-polymer interactions:

1) The following groups, where M^+ and X^- are counterions,

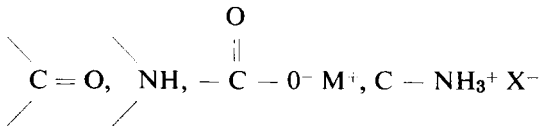

do not form strong interactions with water, a rather controversial finding.

2) 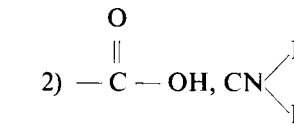 *do* form strong interactions with water.

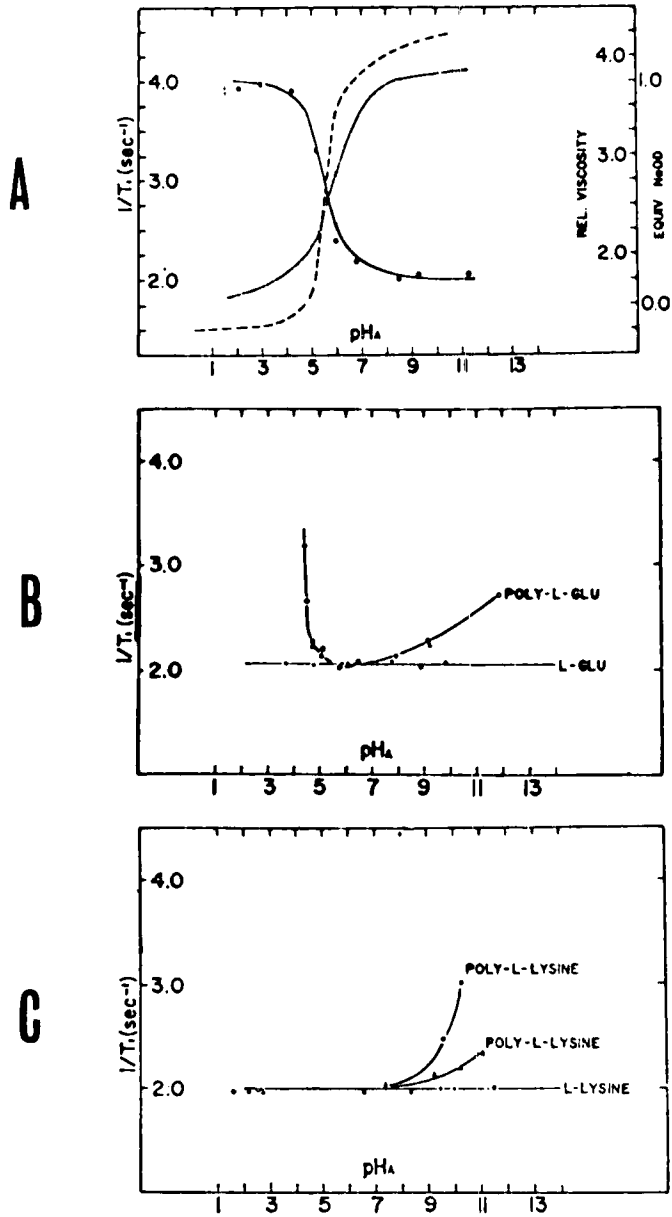

FIGURE 7 (A) Relaxation rate and relative viscosity *vs.* apparent pH, and titration curve of a 3% D_2O solution of poly(methacrylic acid), M = 300,000. (———) Relaxation rate, (— — — —) viscosity, (·····) titration curve. (B) Relaxation rate *vs.* apparent pH for 3% wt/v solutions of poly(L-glutamic acid) and glutamic acid, 0.1 N NaCl in D_2O. (○) M = 100,000; (△) M = 3000. (C) Relaxation rate *vs.* apparent pH for 3% wt/v solutions of poly(L-lysine) and L-lysine, 1 M KBr in D_2O. (○) M = 75,000; (△) M = 5000. Reprinted from Ref. (51) by courtesy of the American Chemical Society.

3) Polymers which have sidechains having formal charges will strongly interact with solvent only if the charges are intra- or intermolecularly wholly or partly neutralized; that is, counterion effects are eliminated.

4) When the conformational fluctuations are large, and have characteristic times of the order of 10^{-3} sec the D_2O-polymer interactions are destroyed.

3 MODELS TO DESCRIBE THE MOLECULAR THERMODYNAMICS OF POLYMER-SOLVENT INTERACTIONS

One of the early attempts to develop a model to describe polymer-solvent interactions was carried out by Nemethy and Scheraga[52] as part of their comprehensive treatment of the structure of water. These workers carried out an extensive investigation of the hydrophobic bond—water interacting with hydrocarbons. Using available data they were able to estimate the experimental values of enthalpy, ΔH_{tr}°, entropy, ΔS_{tr}°, and Gibbs free energy, ΔF_{tr}°, for the transfer of some nonpolar hydrocarbons from the liquid to aqueous solution. These quantities are listed in Table III. Also listed in Table III is a set of computed values of ΔH_{tr}°, ΔS_{tr}° and ΔF_{tr}° made by Nemethy and Scheraga using a solvent-ordering model in which ordered clustering of water molecules was assumed to occur about hydrocarbon molecules. The change in ΔF_{tr}° in going from methane to ethane should correspond roughly to the ΔF_{tr}° of a methyl group while the change in ΔF_{tr}° in going from ethane to propane, or propane to butane, should correspond to the ΔF_{tr}° of a methylene group. This, of course, presupposes conformational variations in the hydrocarbon molecules make constant contributions to ΔH_{tr}° and ΔS_{tr}°.

Later Gibson and Scheraga[53] extended this approach to include polar solute species in aqueous solution and estimated the ΔF_{tr}° of several atoms and groups. These quantities were then used in polymer-solvent model very similar to the hydration shell model which is discussed in detail later in this section.

3.1 Exposure coefficient model

A semi-experimental technique to account for the enthalpy and entropy contributions to the solution stability of collagen, a fibrous protein, as well as collagen triple-helix models, from polymer-solvent interactions was developed by Brown, Hopfinger and Blout.[54] This polymer-solvent interaction model is based upon the concept of exposure coefficients. These coefficients measure the extent to which a solute atom or group which is part of a larger molecule is exposed to the solvent medium. Obviously, the premise here is that the solute interaction with solvent, either favorable or unfavorable, is proportional to the

TABLE III

Observed and calculated thermodynamic parameters for the transfer of normal aliphatic hydrocarbons from the liquid (or nonpolar solution) to aqueous solution at 25°C

	Observed			Calculated		
Substance	ΔF_{tr}° kcal/mol	ΔH_{tr}° kcal/mol	ΔS_{tr}° cal/mol deg	ΔF_{tr}° kcal/mol	ΔH_{tr}° kcal/mol	ΔS_{tr}° cal/mol deg
Methane	+2.51 to +3.15	−2.86 to −2.25	−18.4 to −16.8	+2.60	−1.97	−15.3
Ethane	+3.32 to +3.86	−2.37 to −1.27	−19.5 to −16.8	+3.77	−1.85	−18.8
Propane	+4.90 to +4.91	−2.09 to −1.45	−23.5 to −21.3	+4.96	−1.41	−21.2
Butane	+5.82 to +6.00	−0.96 to −0.72	−22.7 to −21.9	+5.84	−1.18	−23.0

Reprinted from Ref. (52) by courtesy of the American Institute of Physics.

exposure of the solute to the solvent. The solvent-dependent melting equation developed for collagen triple helices is given by

$$T_m = \frac{\sum_{i=0}^{n}\{(n-i)(P_i + \langle U_i\rangle)/n\} - (E_x^R + E_y^R + E_g^R) + \{(m_x^1 + m_y^2 + m_g^3) - [(6-N)+J]\}H^{P-S}}{\frac{1}{2}R \ln(\det \mathbf{F}) - (S_x^R + S_y^R + S_g^R) + \{(m_x^1 + m_y^2 + m_g^3) - [(6-N)+J]\}S^{P-S}} \quad (1)$$

where n refers to the number of tripeptides in each chain, i refers to the ith nearest tripeptide neighbor interaction, P_i is the intra-chain conformational energy for interaction i, $\langle U_i\rangle$ is the average inter-chain conformational energy for interaction i, E_a^R is the average conformational energy for residue a in a random chain, m_a^k is the polymer-solvent exposure coefficient of residue a in the kth position in the tripeptide for the collagen triple helix, N is the number of pyrrolidine ring-containing residues per tripeptide, J is the number of polar sidechain groups per tripeptide, H^{P-S} is the characteristic polymer-solvent interaction enthalpy, $\boldsymbol{R}$ is the gas constant, $\mathbf{F}$ is a matrix having the elements

$$F_{ij} = \frac{\partial^2 E}{\partial u_i\, \partial v_j}\Bigg]_{E = \sum_{k=0}^{n}(P_k + \langle U_k\rangle)}$$

with u_i and v_j being spatial variables which define the triple-helix geometry, S_a^R is the entropy of residue a in a random chain, S^{P-S} is the characteristic polymer-solvent interaction entropy which is sufficiently small for polar solvents, such as water, so as to be neglected, *i.e.*, $S^{P-S} = 0$. All energies and entropies were computed using conformational potential functions as discussed in Ref. 54 except for H^{P-S}, the enthalpy of an "average" interaction of a polar solute species and solvent. H^{P-S} was determined experimentally by insisting that the T_m for some specific biopolymer which is predicted from Eq. (1) for all parameters assigned except H^{P-S}, coincide with the experimentally observed value. Thus H^{P-S} is a calibration parameter. Once a value of H^{P-S} had been determined for a specific biopolymer (Table V references the H^{P-S} calibration biopolymers), that value was retained in all subsequent calculations. The reasonableness of the H^{P-S} values

$H^{P-S} = 2204$ cal/mol of interaction with water

$H^{P-S} = 2112$ cal/mol of interaction with 1,3-propanediol

in view of subsequent studies to be reported here suggests that the assigned energies in Eq. (1) are "in the ballpark". The melting equation for hexapeptides is obtained by adding together numerator terms and denominator terms, respectively, in Eq. (1) for the two tripeptides composing the hexapeptide. This formulation assumes that the ΔH and ΔS cross terms between the unique tripeptides can be arithmetically averaged. This assumption has been substantiated for $(\text{Gly-Pro-Pro-Gly-Pro-Ala})_n$.

Table IV contains the values of the parameters in Eq. (1) for a variety of tripeptides and hexapeptides. Table V contains a listing of observed and predicted melting temperatures for several tripeptides and a couple of hexapeptide collagen triple-helix models in water and 1,3-propanediol.

This formulation demonstrates the importance of the presence and sequencing of proline upon the stability of the triple helix. Moreover, from the predicted and observed melting temperatures in Table V for the polyhexapeptides, it can be seen that when nonproline containing tripeptide sequences

TABLE IV*a*

Triple helix energy and entropy parameters for various tripeptides

Tripeptide	Neighbor (i)	P_1 cal/mol of tripeptide	$\langle U_i \rangle$ cal/mol of tripeptide	$S_{x-y-g}{}^{T}$ cal/mol of tripeptide deg
Pro-Pro-Gly	0	−7000	−4800	
	1	−2400	−1300	9.8
	2	− 300	0	
Pro-Ala-Gly	0	−6400	−5200	
	1	−1400	−1500	18.5
	2	− 200	0	
Ala-Pro-Gly	0	−6600	−5000	
	1	−1400	−1200	19.2
	2	− 200	− 100	
Pro-Ser-Gly	0	−6600	−4800	
	1	−2600	−1600	14.2
	2	− 200	− 100	
Ser-Pro-Gly	0	−6500	−4900	
	1	−1700	−1100	17.6
	2	− 200	− 100	
Ala-Ala-Gly	0	−6400	−5100	
	1	−1700	−1300	25.2
	2	− 100	− 100	
Gly-Pro-Gly	0	−6300	−5000	
	1	−1700	−1300	22.7
	2	0	− 100	
Gly-Ala-Gly	0	−6500	−5100	
	1	−1700	−1400	27.8
	2	− 200	− 100	

TABLE IV*b*

Random-chain energy and entropy parameters

Residue (u)	$E_u{}^{R}$ cal/mol of residue	$S_u{}^{R}$ cal/mol of residue deg
Gly	−3300	10.4
Pro(Hypro)	−2200	3.7
Ala	−2800	8.0
Ser	−2500	7.7

TABLE IV*c*

Exposure coefficients $m_u{}^i$ based on solvent accessibility to a triple-helical structure with coordinates of Yonath and Traub[55] [a]

$m_g{}^1 = 0.9$, $m_p{}^1 = 0.0$	$m_g{}^2 = 1.8$, $m_p{}^2 = 0.8$	$m_g{}^3 = 0.8$
$m_a{}^1 = 0.9$, $m_s{}^1 = 1.7$	$m_{hp}{}^2 = 1.8$, $m_a{}^2 = 1.8$	
	$m_s{}^2 = 2.5$ (water)	

[a] *g* — Gly, *a* — Ala, *p* — Pro, *hp* — Hypro, *s* — Ser.
Reprinted from Ref. (54) by courtesy of Academic Press, Inc.

TABLE V

Comparison of the observed and predicted melting temperatures for some polytripeptide and polyhexapeptide sequences

Polymer	Solvent	*n*	T_m(observed) °C	T_m(predicted) °C
(Pro-Gly-Pro)$_n$[b]	H_2O	22	67	57
	H_2O	100		78
	1,3-propane-diol	22	89	90
	1,3-propane-diol	100		105
(Pro-Pro-Gly)$_n$[c]	H_2O	10	25	25[a]
		15	52	43
		20	65	53
(Pro-Ala-Gly)$_n$[b]	1,3-propane-diol	32	58	58[a]
		55	69	79
(Pro-Ser-Gly)$_n$[b]	1,3-propane-diol	42	51	56
		75	69	63
(Ala-Pro-Gly)$_n$	H_2O	40	—	−60
(Ala-Ala-Gly)$_n$	H_2O	20	—	−169
		40	—	−102
(Ser-Pro-Gly)$_n$	H_2O	40	—	−160
(Gly-Pro-Gly)$_n$	H_2O	40	—	−142
(Gly-Ala-Pro-Gly-Pro-Pro)$_n$[d]	H_2O	17	26	9
		24	32	20
(Gly-Pro-Ala-Gly-Pro-Pro)$_n$[d]	H_2O	12	32	12
		20	41	33
		26	49	40
(Gly-Ala-Ala-Gly-Pro-Pro)$_n$[d]	H_2O	16	19	6
		25	35	25

[a] Calibration values for H^{P-S} (see text).
[b] Brown *et al.*[56]
[c] Kobayashi *et al.*[57]
[d] Segal.[58]
Reprinted from Ref. (54) by courtesy of Academic Press, Inc.

are incorporated into polyhexapeptides adjacent to Pro-X-Gly, X-Pro-Gly, or Pro-Pro-Gly trimers, the melting temperatures of the resulting polyhexapeptides are not simply the arithmetic averages of the melting temperatures of the respective tripeptides. Consideration of the $(Gly\text{-}Ala\text{-}Ala\text{-}Gly\text{-}Pro\text{-}Pro)_n$ melting temperature ($T_m = 25°C$ for $n = 25$), for example indicates that adjacent prolyl residues can stabilize the triple-helical conformation for the entire hexapeptide. As a result, the melting temperature is close to that observed for collagen, and it can be reasoned that the non-triple helix-forming regions (*e.g.*, Ala-Ala-Gly) are stabilized in a collagen-like conformation by their proximity to the more stable proline containing regions. A careful examination of Table V reveals that the thermal stability of the triple helix is markedly influenced by the polarity of the solvent. In general the triple helices are less stable in an aqueous medium than in the less polar 1,3-propanediol solvent. Figure 8 demonstrates the effect of solvent polarity on the thermal stability of the collagen triple helices of varying chain length for three tripeptides.

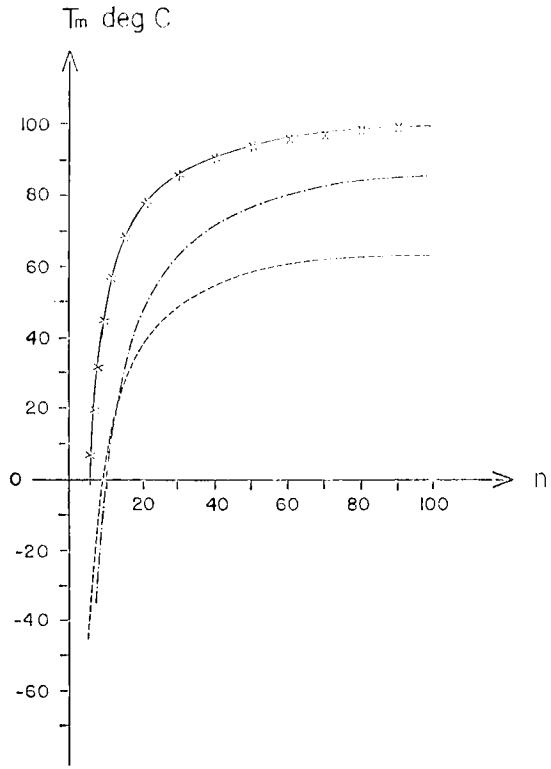

FIGURE 8(a) Melting temperature *vs.* number of polytripeptides per chain, *n*, for the collagen-like triple helix to random state transition in 1,3-propanediol. (————) $(Pro\text{-}Pro\text{-}Gly)_n$; (— · — · —) $(Pro\text{-}Ala\text{-}Gly)_n$; (– – – – – –) $(Pro\text{-}Ser\text{-}Gly)_n$. Reprinted from Ref. (54) by courtesy of Academic Press, Inc.

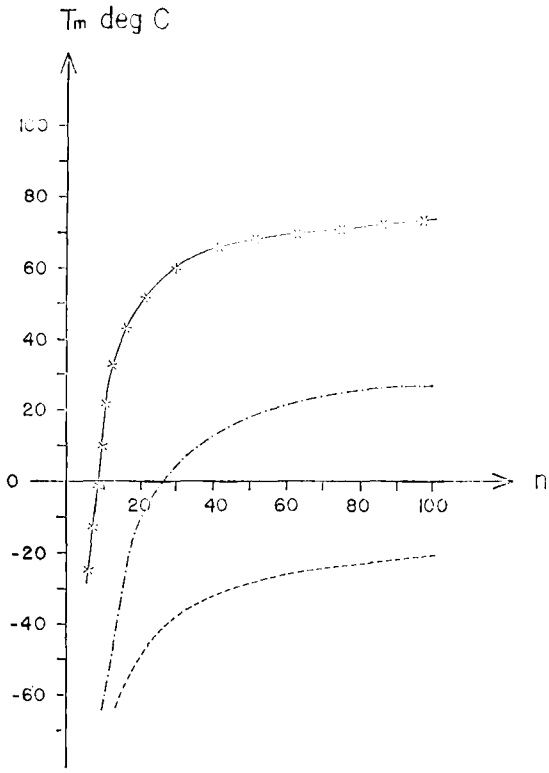

FIGURE 8(b) Melting temperature *vs.* number of polytripeptides per chain, n, for the collagen-like triple helix to random state transition in water. (————) (Pro-Pro-Gly)$_n$; (—·—·—·—·—) (Pro-Ala-Gly)$_n$; (– – – – – – –) (Pro-Ser-Gly)$_n$. Reprinted from Ref. (54) by courtesy of Academic Press, Inc.

Lastly, the model indicates that no single type of interaction is predominantly responsible for the maintenance of the triple helix. Rather, a number of interactions work in unison to stabilize this unique structure.

3.2 The Krimm-Venkatachalam model

The most ambitious theoretical approach to study the effect of water on molecule–polymer interactions has been launched by Krimm and Venkatachalam.[59] These workers have brought water molecules into the vicinity of the carbonyl groups in poly(L-proline) using the geometry shown in Figure 9. By varying the parameters ω, ψ, α and θ they were able to compute the conformational free energies for poly(L-proline). This biopolymer can exist in two forms: Form I, in which adjacent α-carbons are *cis* relative to the imide

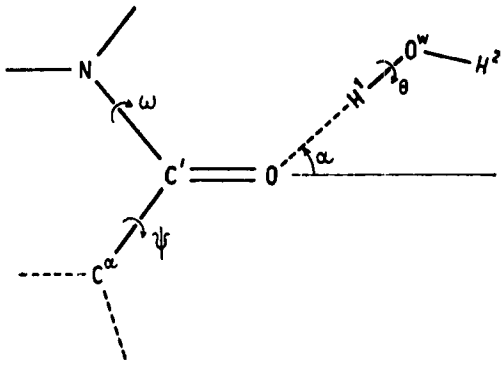

FIGURE 9 Geometry of the imide group with a hydrogen-bonded water molecule.[59]

bond, and Form II, where adjacent α-carbons are *trans* to one another relative to the imide bond. The free energy maps for these two forms of poly(L-proline) with and without water—poly(L-proline) interactions are shown in Figure 10. These results indicate that the *cis* form is nearly independent of interaction with water while the *trans* form of the biopolymer is moderately sensitive to interaction with water. This is in qualitative agreement with experiment.[60]

The disadvantages of this approach to investigating polymer-solvent interactions are (a) the excessive computer time required in the computations to compute free energies due to the large number of degrees of freedom, (b) the neglect of interactions between all groups and/or atoms in the polymer with water molecules.

3.3 The hydration shell model

A general method which circumvents both of these problems is the use of a hydration shell model. We state in advance of describing the hydration shell model that it has the disadvantage of (a) not accounting for possible long-range ordering of solvent molecules about a polymer, (b) introducing several debatable assumptions concerning the molecular energetics of polymer-solvent interactions. Nevertheless, the hydration shell model probably represents the most effective means of dealing with the molecular aspects of polymer-solvent interactions at present.

The concept of a hydration shell to describe the behavior of solvent molecules near a solute species has been used for many years.[61] As mentioned earlier, Gibson and Scheraga[53] modified existing hydration shell models so as to be applicable to the atoms of a solute macromolecule. The model described here is a further modification of the basic hydration shell concept. It differs from the

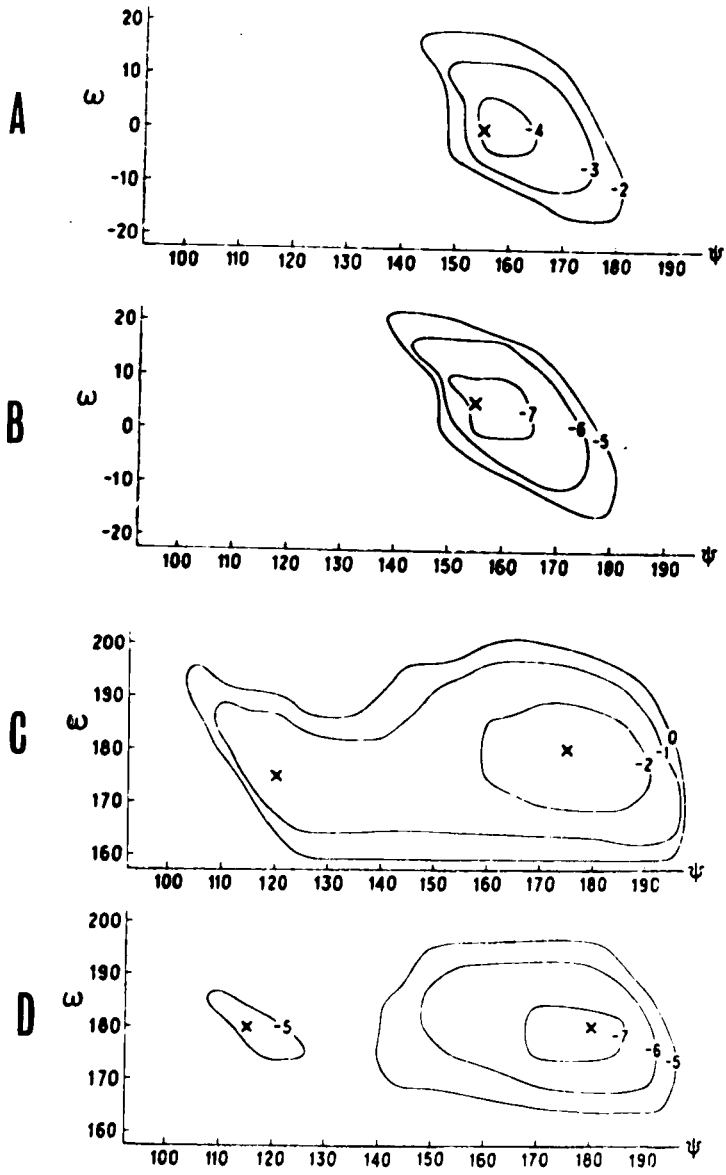

FIGURE 10 Conformational free energy maps of poly(L-proline). (A) *Cis* form without water, (B) *cis* form with water, (C) *trans* form without water, (D) *trans* form with water. Energy contours are in kcal/mol of residue, and × denote minima.[59]

Gibson-Scheraga model in the size and properties of the hydration shells as well as the criteria for calculating excluded volumes.

In adopting a hydration shell model we assume that a characteristic sphere can be centered about each atom of the macromolecule. The size of the sphere, which defines the hydration shell, is dependent upon the solvent molecule and solute atom of the macromolecule. A particular change in free energy is associated with the removal of a solvent molecule from the hydration shell. The size of the hydration shell and the shape of the solvent molecule dictates how many solvent molecules can occupy the hydration shell. The sum of the intersections of the van der Waals volumes of the atoms of the macromolecule with the hydration shell results in an excluded volume which determines how many solvent molecules are removed from the hydration shell when the macromolecule is in a particular conformation. Thus the hydration shell is sensitive to conformation *via* excluded hydration shell volumes.

The hydration shell model is a four parameter system: n = the maximum number of solvent molecules which can occupy the hydration shell; Δf = the change in free energy associated with the removal of one solvent molecule from the hydration shell; R_v = the effective radius of the hydration shell; V_f = the free volume of packing associated with one solvent molecule in the hydration shell.

Table VI contains the values of the parameters n, Δf, R_v and V_f for several different atoms solvated in aqueous solution. Also given in Table VI are the

TABLE VI

The macromolecule-solvent interaction parameters R_v, V_f, n, Δf, and the effective hydration shell volumes V' for some atoms and groups of atoms in aqueous solution.[a]

Atom or group	n	Δf kcal/mol	R_v Å	V_f Å^3	V' Å^3
N(sp^2)	2	.63	4.33	35.8	114.0
C(sp^2)	2	.63	3.90	14.3	71.0
O (carbonyl)	2	1.88	3.94	67.6	177.6
H (amide)	2	.31	3.54	31.3	105.0
CH_3 (aliphatic)	8	−.13	5.50	41.8	498.2
CH_2 (aliphatic)	4	−.10	5.50	60.8	328.0
CH (aliphatic)	2	−.13	5.50	104.8	252.0
CH (aromatic)	3	.11	3.90	3.3	76.6
O (hydroxyl)	2	1.58	3.94	55.2	152.8
H (hydroxyl)	2	.31	3.54	54.7	151.8
O^- (carboxyl)	4	4.20	4.10	42.5	255.0
O (carboxyl)	2	4.20	4.10	64.1	170.6
H (carboxyl)	2	.31	3.54	54.7	151.8

[a]The volume of the H_2O molecule V_s = 21.2 Å^3.

Reprinted from Ref. (65) by courtesy of the American Chemical Society.

values for each V_i' which is defined as the effective volume of the hydration shell of atom i. This quantity must be known in order to compute V_f and, in itself, is a useful parameter for measuring the "amount of room" which solvent molecules can occupy about atom i of the macromolecule. Perhaps the best way to explain how the values of the hydration shell parameters are calculated is to describe the computational procedure for a representative case.

For example, the values of n, R_v, V_f and V' were calculated for N(sp^2) as follows: first, a bonding geometry was assigned to the N(sp^2) atom by choosing a sphere having the van der Waals radius of nitrogen (1.35 Å) to represent the bulk of the atom. Then, to account for the trigonal covalent bonds in which the N(sp^2) atom participates, three cylinders of indefinite length and having a radius equal to three quarters the radius of the sphere were positioned around the van der Waals sphere in three-fold symmetry. The radius of the cylinders was determined from studying space-filling molecular models of N(sp^2). The sphere and cylinders represented an infinite potential barrier to the solvent molecules. The geometry is shown in Figure 11. Solvent molecules were

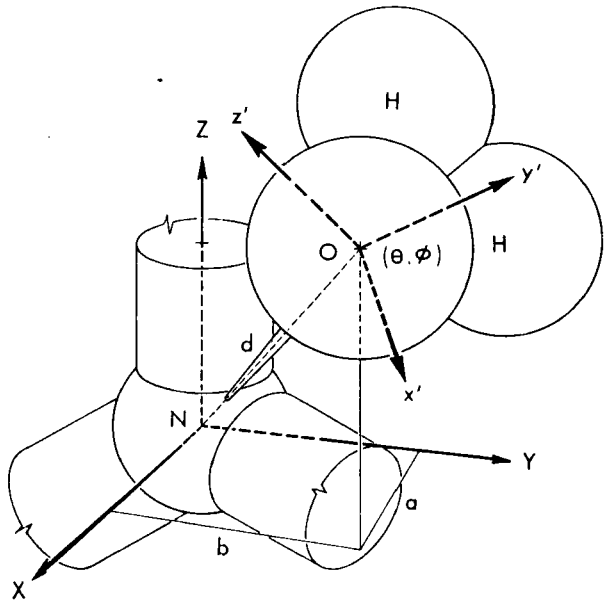

FIGURE 11 Geometry of an N(sp^2) atom in a molecule used to determine the characteristic polymer-solvent interaction parameters using the hydration shell model. Parameter d is the distance of the water molecule from the N atom, and a and b define the position of the water molecule in the XY plane of the N cartesian frame. Angles θ and ϕ define the relative orientation of the water molecule in the cartesian frame associated with the water molecule. Reprinted from Ref. (134) by courtesy of the American Chemical Society.

assigned initial positions about this model for the N(sp^2) atom and the total interaction energy of the system, including interactions between the N(sp^2) atom and solvent molecules as well as solvent molecule–solvent molecule interactions, was minimized using the Davidon technique.[62] Conformational potential functions and parameters described in Ref. 63 were employed to calculate the total interaction energy for each iteration in the minimization. The values of the residual charges on the atoms or groups vary from macromolecule to macromolecule. However, this variation is rather small (< 0.06 electron unit) in all groups reported here. Thus, adopting the residual charges found in polypeptide chains as universally representative of all situations is not too bad an assumption. Whenever possible, use was made of the symmetry of the model in order to reduce the number of variables to be minimized. Since the N(sp^2) atomic geometry possessed a two-fold plane of symmetry (the plane being defined by the axes of the cylinders) solvent molecules were added to the system in pairs of two—one on each side of the plane, and having mirror positions and orientations relative to one another. In order to restrict the calculations to a single hydration shell, the constraint was imposed that only those minima in potential energy were considered which corresponded to positions and orientations of the solvent molecules within a distance equal to the sum of the van der Waals radius[64] for the N(sp^2) atom and the maximum steric diameter of a water molecule (3.7 Å from space-filling models). This distance represents an initial upper-limit approximation for the radius of the hydration shell of the N(sp^2) atom.

The volume, V_s, of the solvent molecule (in this case water) was calculated by assigning van der Waals spheres to represent the oxygen and two hydrogens and determining how much volume these three spheres manifested when they were allowed to overlap in a manner consistent with the bond lengths and bond angle of the H_2O molecule. Equation (6) was used to make this volume calculation, and V_s for H_2O is given in Table VI.

Values of n equal to 2, 4, 6, 8 were used in the energy minimization. The results indicated that $n = 2$ yielded the deepest energy minimum and the two water molecules positioned and orientated themselves about the N(sp^2) atom in such a manner that the effective hydration shell radius, R_v, was 4.33 Å. Next the value of V' was computed by subtracting the volumes of the van der Waals sphere and the three cylinders of the N(sp^2) model from the hydration shell volume of the N$(sp)^2$ atom using R_v as the hydration shell radius. Then, V_f could be computed from

$$V_f = (V' - n\,V_s)/n \tag{2}$$

The free energy of interaction between the solvent molecules and the solute species, f_I, is, obviously, determined in the energy minimization. f_I is a free energy in the sense that the configurational entropy of the various assemblies

of solvent molecules about the solute species is taken into consideration in the calculations. The configurational entropy is computed using the ensemble of states computed in the energy minimization with respect to n, R_v, and V_f. The value of Δf is obtained by subtracting f_1 from the free energy of bulk solvent at $T = 298°K$ determined from Monte Carlo configurational energy calculations on ensembles of solvent molecules. The values of Δf for aqueous solution reported in Table VI are taken from the work of Gibson and Scheraga[53] since these are experimental, rather than theoretical values. It was noted that the theoretical Δf values usually differed from the experimental Δf by about 5% and in no case by more than 12%. This reasonably good agreement between the experimental and theoretical values of the Δf encouraged the theoretical calculation of all the hydration-shell parameters for a number of solvents in addition to water. Table VII lists the hydration-shell parameters for methanol, ethanol, acetic acid, and formic acid. In the calculation of the hydration-shell parameters for ethanol and acetic acid, rotation was allowed about the CH_3—CH_2 and the CH_3—COO(H) bonds, respectively. The conformational energies of these two solvent molecules were calculated as a function of bond rotation by adopting the same potential functions used in the solute-solvent species interactions discussed above.

For acetic and formic acids a decision had to be made concerning the state of ionization of the solvent molecule when interacting with a solute atom or group. The convention was chosen that the neutral form of the acid interacts with those solute species having a negative partial charge, *i.e.*,

TABLE VII

Polymer-solvent parameters for the hydration shell model for a variety of solvents
(A) Formic acid; $V_s = 33.8$ Å^3, *a*—$HCOO^-$, *b*—HCOOH

Atom or group		Δf kcal/mol	R_v Å	V_f Å^3	Molecular species
N(sp^2)	2	1.90	5.80	24.40	*b*
C(sp^2)	2	2.85	5.25	16.50	*a*
O (carbonyl)	2	3.40	5.40	43.80	*b*
H (amide	1	5.95	4.30	22.70	*a*
CH_3 (aliphatic)	6	−.09	5.95	30.75	*a*
CH_2 (aliphatic)	4	−.08	5.95	28.60	*a*
CH (aliphatic)	1	.06	5.75	15.75	*a*
CH (aromatic)	2	.08	4.45	19.00	*a*
O (hydroxyl)	1	2.55	4.85	40.60	*b*
H (hydroxyl)	1	4.75	4.30	43.95	*a*
O^- (carboxyl)	3	5.05	5.85	29.75	*b*
O (carboxyl)	1	3.55	5.20	18.50	*b*
H (carboxyl)	1	3.55	5.20	18.50	*b*

TABLE VII—*continued*

(B) Acetic acid; $V_s = 51.6$Å^3, *a*—H_3CCOO^-, *b*—H_3CCOOH

Atom or group	*n*	Δf kcal/mol	R_v Å	V_f Å$_3$	Molecular species
N(sp^2)	2	1.95	6.60	48.75	*b*
C(sp^2)	2	2.85	5.60	39.80	*a*
O (carbonyl)	2	3.35	5.80	96.50	*b*
H (amide)	1	5.85	4.90	47.35	*a*
CH_3 (aliphatic)	6	−.08	6.20	31.60	*a*
CH_2 (aliphatic)	4	−.08	6.20	35.83	*a*
CH (aliphatic)	1	.06	5.95	18.98	*a*
CH (aromatic)	2	.08	4.65	22.07	*a*
O (hydroxyl)	1	2.55	5.80	48.60	*b*
H (hydroxyl)	1	4.55	4.90	67.40	*a*
O^- (carboxyl)	3	4.96	6.60	49.50	*b*
O (carboxyl)	1	3.45	6.10	33.70	*b*
H (carboxyl)	1	3.45	6.10	33.70	*b*

(C) Methanol; $V_s = 42.8$ Å^3

Atom or group	*n*	Δf kcal/mol	R_v Å	V_f Å^3
N(sp^2)	2	.23	4.70	41.6
C(sp^2)	2	.18	5.20	53.6
O (carbonyl)	2	1.45	4.80	43.9
H (amide)	1	.30	4.10	30.5
CH_3 (aliphatic)	4	.38	5.90	19.5
CH_2 (aliphatic)	3	.32	5.70	21.6
CH (aliphatic)	2	.32	5.70	21.6
CH (aromatic	2	.46	4.70	28.5
O (hydroxyl)	1	.85	3.65	38.8
H (hydroxyl)	1	.85	3.65	38.8
O^- (carboxyl)	2	2.80	4.80	48.5
O (carboxyl)	1	1.30	4.35	28.6
H (carboxyl)	1	1.15	4.35	29.3

(D) Ethanol; $V_s = 63.7$ Å^3

Atom or group	*n*	Δf kcal/mol	R_v Å	V_f Å^3
N(sp^2)	2	.18	6.20	49.8
C(sp^2)	2	.15	5.80	57.5
O (carbonyl)	2	1.18	6.20	49.1
H (amide)	1	.28	5.50	45.6
CH_3 (aliphatic)	4	.41	7.10	31.3
CH_2 (aliphatic)	3	.39	7.00	31.8
CH (aliphatic)	2	.39	6.90	33.0
CH (aromatic)	2	.40	6.35	42.9
O (hydroxyl)	1	.57	4.15	51.6
H (hydroxyl)	1	.57	4.20	51.6
O^- (carboxyl)	2	2.45	6.35	60.7
O (carboxyl)	1	1.10	5.90	43.5
H (carboxyl)	1	.88	5.90	43.5

Reprinted from Ref. (134) by courtesy of the American Chemical Society.

interactions of the type

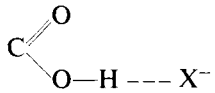

and the charged form of the acid interacts with those solute species possessing a positive partial charge, *i.e.*, interactions of the type

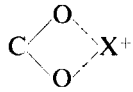

Mechanistically this scheme of interactions would correspond to a solute molecule in a solution of completely ionized acid. The ionized acid molecules would interact with the groups of the solute molecule having positive partial charge. The free protons would interact with the groups of the solute molecules having negative partial charges. In turn, the ionized acid molecules would interact with the proton-negative charge group complexes. This last interaction should be similar to the neutral form of the acid molecule interacting with solute groups having partial charges. In Table VII a distinction is made concerning which form of the acid is used to compute the hydration-shell parameters for each solute species. The values of V_s for each of these solvent molecules were determined in the same manner as for water.

To complete the polymer-solvent interaction model the following properties are assigned to the hydration shells:

i) Each solvent molecule occupies an identical volume, $(V_s + V_f)$, in a hydration shell which is independent of how many other solvent molecules are present at any instant.

ii) The dynamic characteristic of the polymer-solvent interaction is included by *assuming* a *linear* relationship between the total change in free energy and the amount of excluded volume in the hydration shell.

iii) There is no additional contribution to the polymer-solvent free energy from a hydration shell once n solvent molecules have been removed from the hydration shell.

iv) All energy parameters are temperature independent and valid only near room temperature.

There are three unique types of intersections between the hydration shell of atom i and the van der Waals sphere of atom j having volume v_j and radius r_j:

i) $V_i' \cap v_j = 0$ when $(R_v)_i + r_j \leq r_{ij}$ where r_{ij} is the distance between the centers of atom i and atom j.

ii) $V_i' \cap v_j = 4/3\ \pi\ r_j^3$ when $r_j + r_{ij} \leq (R_v)_i$.

iii) The third case is $(R_v)_i + r_j > r_{ij}$. With the aid of Figure 12 we can derive

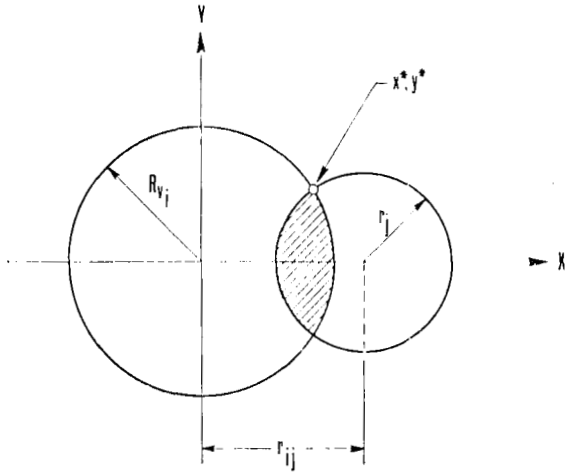

FIGURE 12 A two-dimensional projection of the geometry of the intersection of the solvation shell of atom *i* and the van der Waals sphere of atom *j*. From Ref. (65) by courtesy of the American Chemical Society.

an expression for $V_i' \cap v_j$. First we compute the volume associated with $V_i' \cup v_j$ by the solid of revolution technique. From simple analytic geometry it is found that the x-coordinate, x^*, of the intersection of the solvation shell and the van der Waals sphere is given by,

$$x^* = \frac{(R_v)_i^2 - r_j^2 + r_{ij}^2}{2r_{ij}} \tag{3}$$

Then for $r_j + (R_v)_i > r_{ij}$

$$V_i' \cup v_j = \pi \left[\int_{-(R_v)_i}^{x^*} [(R_v)_i^2 - x^2]dx + \int_{x^*}^{r_j + r_{ij}} (r_j^2 - [x - r_{ij}]^2)dx \right] \tag{4}$$

and

$$V_i' \cap v_j = (4/3)\,\pi\,[(R_v)_i^3 + r_j^3] - V_i' \cup v_j \tag{5}$$

or,

$$V_i' \cap v_j = (\pi/3)\,[2(R_v)_i^3 + 2r_j^3 + r_{ij}^3] - \pi\,[(R_v)_i^2\,x^* + (r_{ij} - x^*)\,(r_j^2 + r_{ij}\,x^*)] \tag{6}$$

Then for some particular conformation, K, of the macromolecule having a total of N atoms the total excluded volume of the ith hydration shell due to all other nonbonded atoms is

$$V_i^\circ = \sum_{j \neq i}^{N} (V_i' \cap v_j) \tag{7}$$

where i and j are not bonded. Since the solvation free energy is, in terms of this

model, the change in free energy in going from a completely solvated state to some partially solvated state dictated by conformation K, the total solvation free energy, $F_i(K)$, associated with atom i in the Kth conformation is

$$F_i(K) = \Delta f \left(n - \frac{V_i^\circ}{V_s + V_f} \right) \text{ if } V_i^\circ < n(V_s + V_f) \tag{8}$$

$$F_i(K) = 0 \qquad \text{if } V_i^\circ \geq n(V_s + V_f) \tag{9}$$

where n, Δf, and V_f are chosen according to which type of atom is indicated by the index i.

From the way $F_i(K)$ is defined in Eqs. (8) and (9), it is clear that $F_i(K)$ has a discontinuous first derivative for $V_i^\circ = n(V_s + V_f)$. However, since we are considering the intersection of spheres with spheres, V_i° will never equal $n(V_s + V_f)$ unless there is a steric overlap of the van der Waals spheres. Under such conditions the conformational energy will be exceedingly high and the entire structure will be rejected. Hence, this polymer-solvent model has continuous energy functions for all "sterically" allowed polymer conformations and can be used without fear of "blow ups" in any minimization routine.

The total solvation free energy, $F_T(K)$, for the macromolecule in the Kth conformation is simply:

$$F_T(K) = \sum_{i=1}^{N} F_i(K) \tag{10}$$

3.4 Polymer-solvent studies using the hydration shell model

In this section two types of polymer-solvent studies using the hydration shell model are reported. In the first investigation aqueous solution–polypeptide interactions were considered as part of a conformational study of a variety of polypeptides having chemically and structurally different side chains. In the second study a series of solvent-dependent conformational energy computations were carried out for oligomeric and polymeric forms of poly(L-alanine) and poly(L-proline) in a variety of simple solvents.

3.4.1 Homopolypeptides in aqueous solution

Table VIII contains the values of the free energies $<A>$, average internal energies $\bar{E}$, and entropies $<S>$ for a number of polypeptides in and out of aqueous solution.[65] Some conclusions, which can be considered possibly valid only for polar solvents have been postulated from these calculations. Further, since the size and shape of the solvent molecule appears to be as important as its polarity (see next section) in defining the characteristic interaction with

TABLE VIII

Free energies $\langle A \rangle$, average internal energies $\bar{E}$, and entropies $\langle S \rangle$ associated with different conformations of several homopolypeptides[a]

	$\langle A \rangle$, kcal/mol of residue			$\bar{E}$, kcal/mol of residue			$\langle S \rangle$, cal/(mol of residue deg)		
	Aqueous solution	Vacuum	ΔA(PS)	Aqueous solution	Vacuum	$\Delta \bar{E}$ (PS)	Aqueous solution	Vacuum	ΔS (PS)
				Poly(L-alanine)					
α_R[b]	−5.5	−5.4	−0.1	−4.3	−4.4	+0.1	3.56	3.40	0.16
β卌[c]	−3.4	−3.1	−0.3	−1.6	−1.2	−0.4	5.94	6.57	−0.63
PPII[d]	−4.2	−3.6	−0.6	−2.5	−1.6	−0.9	5.68	6.31	−0.63
				Poly(L-proline)					
PPII	−1.7	−1.1	−0.6	0.0	0.5	−0.5	5.74	5.29	−0.45
				Poly(L-valine)					
α_R	12.3	11.7	+0.6	12.3	11.7	+0.6	0.00	0.00	0.00
β卌	−2.0	−2.3	+0.3	−0.9	−1.3	+0.4	3.75	3.78	−0.03
PPII	0.9	0.0	+0.9	1.9	0.8	+1.1	3.03	2.50	+0.53
ECF[e]	−2.7	−2.9	+0.2	−1.6	−1.8	+0.2	3.74	3.73	+0.01
				Poly(L-serine)					
α_R	−0.3	+2.5	−2.8	−0.0	2.8	−2.8	0.90	1.03	−0.13
β卌	3.9	−0.3	−3.6	−3.2	0.3	−4.1	2.29	2.05	+0.24
PPII	−2.7	+0.8	−3.5	−2.1	1.3	−3.3	1.85	1.47	+0.38
				Poly(L-aspartic acid) Neutral Form					
α_R	−19.5	−5.1	−14.4	−19.3	−4.8	−14.5	0.67	1.03	−0.36
β卌	−18.8	+0.5	−19.3	−18.4	+1.3	−19.7	1.57	2.86	−1.29
PPII	−19.3	−1.6	−17.7	−18.9	−1.1	17.8	1.39	1.88	−0.49
ECF	−14.2	+1.2	−15.4	−13.9	+1.4	−15.3	0.94	0.73	−0.12
				Poly(L-aspartic acid) Charged Form					
α_R	−7.8	+19.8	−27.6	−7.5	+20.2	−27.7	1.05	1.25	−0.20
β卌	−1.4	+22.3	−23.7	−0.7	+22.9	−23.6	2.09	2.19	−0.10
PPII	−4.7	+26.7	−22.0	−5.3	+27.6	−22.3	1.95	3.08	−1.13
ECF	+3.6	+24.5	−20.9	+4.3	+25.1	−20.8	2.44	1.95	+0.49

				Poly(L-glutamic acid) Neutral Form					
α_R	−0.3	+12.1	−12.4	+0.2	12.7	−12.9	1.46	2.45	−0.99
β ⋕	1.7	+17.1	−18.9	+0.6	20.1	−20.7	3.55	4.03	−0.48
PPII	1.6	−17.1	−18.7	+0.4	20.2	−20.6	3.61	5.27	−1.66
ECF	1.4	+16.8	−18.2	+0.2	20.0	−20.2	3.77	5.95	−21.8
				Poly(L-glutamic acid) Charged Form					
α_R	−4.1	+20.0	−24.1	−3.6	+21.0	−25.6	1.50	3.40	−1.90
β ⋕	−12.4	+11.8	−24.2	−11.5	+13.1	−24.6	3.22	4.15	−0.93
PPII	−15.7	+10.6	−26.3	−14.6	+12.2	−26.8	3.50	5.40	−19.0
ECF	−20.9	+9.0	−20.9	−19.8	+10.7	−30.5	3.51	5.60	−2.09
				Poly(L-histidine) Neutral Form					
α_R	−8.8	−7.6	−1.2	−8.3	−7.1	−1.2	1.41	1.41	0.00
β ⋕	−6.8	−4.8	−2.0	−6.2	−4.2	−2.0	2.00	2.11	−0.11
PPII	−6.5	−4.5	−2.0	−6.0	−4.1	−1.9	1.74	1.65	+0.09
				Poly(L-histidine) Charged Form					
α_R	−2.3	+7.4	−5.1	2.9	8.0	−5.1	1.95	1.90	0.05
β ⋕	−2.8	+4.2	−7.0	−2.2	4.9	−7.1	2.10	2.50	−0.40
PPII	−3.5	−3.1	−6.6	−2.9	3.8	−6.7	1.98	2.25	−0.27
ECF	−1.6	+5.3	−6.9	−0.9	6.0	−6.9	2.40	2.43	−0.03
				Poly(L-lysine) Neutral Form					
α_R	−5.8	−5.2	−0.6	−4.5	−4.0	−0.5	4.15	3.95	−0.20
β ⋕	−0.9	−0.2	−0.7	+0.7	1.5	−0.8	5.41	5.68	−0.27
PPII	−0.3	+1.0	−1.0	+2.0	3.0	−1.0	4.85	6.40	−0.55
ECF	−0.4	+0.7	−1.1	+1.3	2.4	+1.1	5.76	6.13	−0.37
				Poly(L-lysine) Charged Form					
α_R	−1.1	+6.5	−7.6	0.0	7.6	−7.6	3.65	3.50	+0.15
β ⋕	−2.3	+5.8	−8.1	−0.8	7.5	−8.3	5.13	5.71	−0.58
PPII	−3.7	+4.3	−8.0	−2.1	6.0	−8.1	5.41	5.83	−0.42
ECF	−1.9	+6.0	−7.9	−0.5	7.5	−8.0	4.70	5.02	−0.32

[a] $\langle A \rangle$, $\bar{E}$ and $\langle S \rangle$ are given for both aqueous solution and vacuum. The changes in free energies, ΔA(PS), average internal energies, $\Delta \bar{E}$(PS), and entropies, ΔS(PS), in going from the vacuum to aqueous solution are also listed. The temperature was fixed at 298°K. [b] Right-handed α helix. [c] Antiparallel β sheet. [d] Poly(L-proline) II helix. [e] Extended charged-form helix.

Reprinted from Ref. (65) by courtesy of the American Chemical Society.

solute molecules, care must be taken in adopting the findings reported here to *all* types of polar solvents. The conclusions are:

i) For polar solvents, such as water, the interactions of polar groups in the macromolecule with solvent are much more stabilizing than the hydrophobic group interactions with solvent are destabilizing. Poly(L-valine) has a destabilization free energy in aqueous solution (as compared to vacuum) of about 0.5 kcal/mol of residue while poly(L-aspartic acid) in the neutral form has a stabilization free energy in aqueous solution (as compared to vacuum) of around 17 kcal/mol of residue.

ii) The change in polymer-solvent free energy in going from a polar solvent to vacuum (neutral solvent) is roughly proportional to the solubility of the polymer. Those homopolypeptides which have charged side chains are most soluble. The higher the hydrophobic character of the homopolypeptide the lower the solubility. Poly(L-proline) in form II probably should have a higher ΔA(PS) in view of its known high solubility in aqueous solution. This suggests that the Δf's needed to describe the carbonyl carbon and oxygen polymer-solvent interactions for imino acids might be different from the Δf's used for carbonyl carbon and oxygen polymer-solvent interactions used for amino acids.

iii) The polymer-solvent interaction free energy is dependent upon the conformation of the polymer backbone and the size and chemical nature of the polymer side chain. Poly(L-alanine) would be more soluble (in aqueous solution) in a PP II conformation than in a right-handed α helix. However, from a comparison of the conformational free energies it can be seen that right-handed α helix is statistically more probable. Thus, maximum water-solubility of poly(L-alanine) is diminished by conformational restrictions.

iv) The polymer-solvent interactions (in this case strictly for aqueous solution and homopolypeptides) do not change the ranking of the conformations of non-ionizable homopolypeptides with respect to stability relative to the vacuum calculations. However, the statistical weights associated with observing the various conformations are sensitive to polymer-solvent interactions. In general, the right-handed α helix becomes less probable while the other conformations become more probable when aqueous solution-homopolypeptide interactions are included in the calculations. Figures 13 (f) and (h) in the next section are conformational (ϕ,ψ) maps for poly(L-alanine) based on vacuum calculations and aqueous solution-homopolypeptide calculations, respectively. The region in the upper left hand corner of the map increases in stability for aqueous solution–poly(L-alanine) interactions at the expense of the right-handed α-helical region, $\phi = 130°$, $\psi = 120°$. Thus, if one attempts

to use conformational calculations to predict Boltzmann average properties of a macromolecule (*e.g.*, spectra, transition temperatures) in aqueous solution, it is important to be sure that the polymer-solvent interactions are included in the computations. Hence, Aebersold and Pysh[66] were not able to accurately predict the statistical average CD spectra of various homopolypeptides perhaps because they neglected polymer-solvent interactions, and not because of major errors in the conformational potential functions. Polymer-solvent interactions may cause major changes in the conformations of heteropolypeptide chains which contain a mixture of polar and hydrophobic groups (*i.e.*, proteins) and are in aqueous solution. The effects of polymer-solvent interactions are maximized under these conditions.

v) Aqueous solution-homopolypeptide interactions for homopolypeptides having ionizable side chains are extremely stabilizing (10–30 kcal/mol of residue). Hence we should expect that these interactions are extremely important in dictating the conformational properties of such macromolecules.

3.4.2 Poly (L-alanine) and poly (L-proline) in different solvents

In this series of calculations the chain properties of poly(L-alanine) and poly(L-proline) were determined as a function of solvent and *ordered* chain-length. The same potential functions discussed in Ref. 63, as mentioned earlier, were used in computation of the energies reported here. In the case of poly-(L-proline), rotation was allowed about the imide bond, which is denoted by ω ($\omega = 180^\circ$ corresponds to the *trans* configuration). The torsional potential about this partial double bond is described in Ref. 67.

If k is the number of residues which compose the polypeptide chain, then the mean square axial length of an ordered chain segment is:

$$\langle l_k^2 \rangle = \sum_{i=1}^{N} (k\hat{l}_i')^2 P_i^{(k)} = k^2 \sum_{i=1}^{N} \hat{l}_i'^2 P_i^{(k)} = k^2 \langle \hat{l}_k^2 \rangle \tag{11}$$

where N is the number of conformational states considered in the averaging process, and $\hat{l}_i'$ is the axial length, relative to the helix generated by conformation i, of a residue unit. In the calculations reported here, end effects, due to carboxyl and amine groups, are not considered. In other words, we deal here with a chain segment located in the "middle" of a long chain molecule. The quantity $P_i^{(k)}$ is the probability of observing the ith conformation for a k-mer,

$$P_i^{(k)} = \frac{\exp(-E_i^{(k)}/RT)}{\sum_{j=1}^{N} \exp(-E_j^{(k)}/RT)} \tag{12}$$

where $E_j^{(k)}$ is the total conformational energy of state j. The energy $E_j^{(k)}$ can be expressed in terms of the sum of the pairwise residue–residue neighbor interactions,

$$E_j^{(k)} = k\,E_j(0) + (k-1)E_j(1) + (k-2)E_j(2) + \ldots + E_j(k-1) = \sum_{i=0}^{k}(k-i)E_j(i) \tag{13}$$

where $E_j(i)$ is the interaction energy between ith nearest-neighbor residues each of which are in the jth conformational state. Only the first six nearest-neighbor residue–residue interactions were considered in the calculations reported here,

$$E_j^{(k)} \approx \sum_{i=0}^{6}(k-i)E_j(i) \quad \text{for } k > 6. \tag{14}$$

L-alanine

In Figure 13 are shown the digitalized conformational maps for two planar-peptide units of L-alanine and for a long ordered chain of L-alanine planar-peptide units (LCA). The dipeptide calculations correspond to the least ordered chain, *i.e.*, it is a model for the "random coil" of L-alanine (RCA)[68] while the long chain corresponds to the completely ordered polymer. Thus these two maps, for each choice of solvent, should describe the conformational properties of the least and most ordered forms of poly(L-alanine). For the sake of space, the other conformational energy maps are not presented here.

The RCA maps indicate that the most probable conformations of the dipeptide unit of L-alanine are either β or left-handed 3_1 helix in all solvents. In vacuum, as noted in other studies,[69] the 2_1 helix ($\phi = -80°$, $\psi = 100°$) is the most probable structure. An interesting observation, which persists for longer oligomeric chains, is that the larger solvent molecules, ethanol and acetic acid, promote the formation of the left-handed 3_1-helical structure while water, methanol and formic acid, less bulky solvent molecules, aid in the formation of β conformations. In this regard, solvent polarity has little effect. These findings would suggest that a polymer of RCA could be rather unordered, but yield CD/ORD spectra indicative of a β- or left-handed 3_1-helical structure.

The overall topologies of the conformational energy surfaces of the dipeptides of L-alanine are very similar in all solvents. There is a significantly greater degree of conformational freedom in these maps as compared to those of LCA. The interactions between polymer and solvent have a large stabilizing effect for acetic acid and formic acid as would be expected. Water, which is relatively polar when compared to methanol and ethanol, surprisingly has

Part a. The lowest energy is −9.8 kcal/mol per dipeptide, located at (−160,140), for the dialanine chain in methanol

180	−7.5	−9.0	−8.7	−8.0	−7.9	−7.9	−6.6						−5.6	−1.8				−2.7	−7.5
160	−8.0	−9.4	−8.8	−8.3	−8.3	−8 3	−8.0	−0.5					−1.5	−1.8				−3.1	−8.0
140	−8.4	−9.8	−9.1	−8.4	−8.4	−8.4	−8.3	−6.9						−1.3				−3.2	−8.4
120	−8.0	−9.5	−8.7	−8.1	−8.3	−8.5	−8.4	−7.5	−0.3					−0.7				−2.7	−8.0
100	−7.6	−9.1	−8.4	−7.9	−8.4	−8.9	−8.0	−5.5	−1.2				−1.7	−0.6				−2.3	−7.6
80	−7.3	−8.8	−8.1	−7.7	−8.5	−7.9						−3.1	−4.9	−0.5				−2.0	−7.3
60	−7.1	−8.5	−7.9	−7.6	−8.5	−5.3					−1.1	−6.6	−5.6	−0.6				−1.9	−7.1
40	−6.9	−8.4	−7.7	−7.4	−8.1	−6.0						−7.2	−6.2	−0.9				−1.5	−6.9
20	−4.5	−7.4	−7.2	−6.8	−7.3	−7.2							−6.5	−1.0					−4.5
0		−3.4	−6.1	−6.2	−6.6	−7.1	−4.3						−3.8	−1.4					
−20	−5.0	−5.2	−6.2	−6.6	−7.0	−7.3	−7.6							−2.0				−1.6	−5.0
−40	−7.8	−8.9	−8.0	−7.4	−7.6	−7.7	−7.8	−7.4						−1.3				−2.9	−7.8
−60	−8.0	−9.1	−8.1	−7.3	−7.4	−7.4	−7.3	−6.8	−1.7					−0.6				−3.1	−8.0
−80	−7.5	−8.5	−7.5	−6.7	−6.7	−6.7	−5.8	−2.7						−2.4				−2.6	−7.5
−100	−6.5	−7.5	−6.5	−5.6	−5.6	−5.4	−1.4					−4.9	−6.1	−1.9				−1.6	−6.5
−120	−5.9	−6.9	−5.8	−4.9	−5.0	−4.6						−5.9	−5.4	−0.4				−1.0	−5.9
−140	−6.8	−7.9	−6.8	−5.9	−6.0	−5.7						−5.6	−5.7	−0.8				−1.8	−6.8
−160	−7.3	−8.7	−8.1	−7.2	−7.2	−7.1	−1.7					0 0	−6.2	−1.5				−2.2	−7.3
−180	−7.5	−9.0	−8.7	−8.0	−7.9	−7.9	−6.6						−5.6	−1.8				−2.7	−7.5
	−180	−160	−140	−120	−100	−80	−60	−40	−20	0	20	40	60	80	100	120	140	160	180

FIGURE 13 Digitalized conformational energy maps for dipeptide L-alanine and for (L-alanine)$_{50}$ which is chosen as a model for the polymer, in five solvents and *in vacuo*. The angle ϕ is plotted along the abscissa, and Ψ along the ordinate. The total conformational energy was minimized with respect to χ_1 at each point. The energies left blank are greater than 5 kcal/mol of residue above the minimum. Reprinted from Ref. (134) by courtesy of the American Chemical Society.

Part b. The lowest energy is 2.6 kcal/mol per residue, located at (−60, −40), for the infinite alanine chain in methanol

	−180	−160	−140	−120	−100	−80	−60	−40	−20	20	40	60	80	100	120	140	160	180
180	6.6	5.8	4.8	5.4	5.3	6.6												6.6
160	5.9	4.4	4.7	5.1	4.3	4.7	5.9											5.9
140	4.4	3.8	4.3	5.0	4.2	3.6	4.5	6.0									7.0	4.4
120	4.6	4.0	4.3	4.9	4.3	4.7	5.4	4.9										4.6
100	6.0	3.5	3.9	4.3	4.8	5.6	5.9											6.0
80	5.1	5.4	5.8	4.1	5.0	6.5												5.1
60	6.0	5.0	6.0	7.8	7.2						4.6							6.0
40	6.2	5.1	5.2	5.2	5.9							3.8						6.2
20			6.1	6.3	5.9	5.5						4.1						
0					7.1	5.2	7.1					7.4						
−20					6.9	5.0	3.4											
−40	5.2	5.0	5.7														7.5	5.2
−60	5.1	4.9	5.4	6.1				4.2									7 5	5.1
−80	5.0	4.7																5.0
−100												7.2						
−120											6.7	7.7						
−140												6.4						
−160		6.1	5.4	6.1	6.1	6.2						6.9						
−180	6.6	5.8	4.8	5.4	5.3	6.6												6.6

FIGURE 13 *continued*

Part c. The lowest energy is −11.0 kcal/mol per dipeptide, located at (−80,120), for the dialanine chain in ethanol

	−180	−160	−140	−120	−100	−80	−60	−40	−20	0	20	40	60	80	100	120	140	160	180
180	−7.3	−8.7	−8.4	−8.2	−9.0	−9.8	−7.4						−6.4	−3.5				−2.4	−7.3
160	−7.7	−8.9	−8.6	−8.4	−9.2	−9.8	−9.1	−1.7					−2.1	−2.5				−2.8	−7.7
140	−7.8	−9.0	−8.5	−8.4	−9.2	−9.8	−10.5	−8.0						−1.8				−2.7	−7.8
120	−7.9	−9.0	−8.7	−8.7	−9.7	−11.0	−10.3	−9.1	−2.3					−1.6				−2.7	−7.9
100	−7.9	−9.3	−8.9	−9.0	−10.2	−10.7	−10.1	−7.8	−3.3				−2.7	−1.9				−3.1	−7.9
80	−8.3	−9.8	−9.4	−9.6	−10.6	−10.2					−1.8	−5.2	−6.4	−2.2				−3.0	−8.3
60	−7.8	−9.4	−9.0	−9.3	−10.2	−7.4					−2.6	−8.3	−7.3	−2.7				−2.5	−7.8
40	−7.5	−9.0	−8.6	−9.0	−9.9	−7.9						−8.6	−8.7	−2.6				−2.1	−7.5
20	−5.1	−8.1	−8.1	−8.2	−9.0	−9.1						−1.7	−8.0	−2.9					−5.1
0		−3.9	−6.8	−7.3	−8.4	−9.1	−6.3						−5.2	−2.9					
−20	−5.1	−5.3	−6.4	−7.3	−8.3	−9.2	−9.1	−1.8						−3.0				−1.7	−5.1
−40	−8.0	−9.0	−8.4	−8.2	−8.9	−9.5	−10.3	−9.1						−2.3				−3.2	−8.0
−60	−8.4	−9.5	−8.8	−8.4	−9.0	−9.7	−9.0	−8.9	−3.7					−1.9				−3.6	−8.4
−80	−8.3	−9.4	−8.7	−8.3	−9.0	−8.7	−7.6	−5.2	−2.2					−4.1				−3.5	−8.3
−100	−6.8	−8.3	−7.5	−7.2	−7.8	−7.2	−2.8				−1.8	−6.9	−8.2	−3.5				−1.9	−6.8
−120	−5.9	−7.1	−6.4	−6.4	−7.1	−6.1						−7.6	−7.7	−2.9				−1.0	−5.9
−140	−6.7	−7.8	−7.2	−6.9	−8.1	−7.1						−7.2	−8.6	−2.6				−1.7	−6.7
−160	−7.1	−8.5	−8.0	−7.8	−8.5	−8.3	−2.6					−1.6	−7.6	−3.1				−2.1	−7.1
−180	−7.3	−8.7	−8.4	−8.2	−9.0	−9.8	−7.4						−6.4	−3.5				−2.4	−7.3

FIGURE 13 *continued*

Part d. The lowest energy is 3.3 kcal/mol per residue, located at (−80,140) and (−60,−40), for the infinite alanine chain in ethanol

	−180	−160	−140	−120	−100	−80	−60	−40	−20	0	20	40	60	80	100	120	140	160	180
180	7.1	6.3	5.4	5.6	4.8	5.7													7.1
160	6.6	5.2	5.3	5.5	4.0	4.2	6.3												6.6
140	5.4	5.0	5.4	5.7	4.2	3.3	4.1	6.9										7.9	5.4
120	5.2	4.6	5.0	5.2	3.9	3.5	5.3	5.1											5.2
100	6.2	3.9	4.2	4.3	4.2	5.0	5.7	7.8										7.5	6.2
80	4.7	5.0	5.3	3.5	4.3	5.5												7.6	4.7
60	6.0	5.0	6.1	7.6	7.1							6.1							6.0
40	6.6	5.5	5.7	5.4	5.8	7.8							4.5						6.6
20		7.0	7.0	7.0	6.2	5.7							4.6						
				8.3	7.2	5.7	7.6						8.2						
−20					6.8	5.4	4.6												
−40	6.0	5.9	6.7				3.3											8.2	6.0
−60	5.5	5.4	6.1	7.0				5.3										7.8	5.5
−80	4.9	4.7																	4.9
−100													7.1						
−120												7.7	7.6						
−140													5.6	7.5					
−160	7.2	6.4	5.6	5.9	5.3	6.0							7.4	7.9					7.2
−180	7.1	6.3	5.4	5.6	4.8	5.7													7.1

FIGURE 13 *continued*

Part e. The lowest energy is −2.3 kcal/mol per dipeptide, located at (−80,100), for the dialanine chain *in vacuo*

180	0.0	−1.0	−1.0	−0.5	−0.8	−0.9	−0.4					0.9	4.7				4.9	0.0
160	−0.3	−1.2	−1.2	−0.8	−1.1	−1.4	−1.1	6.3				5.1	5.0				4.6	−0.3
140	−0.6	−1.5	−1.3	−0.9	−1.3	−1.7	−1.7	−0.2					5.6				4.6	−0.6
120	0.4	−1.5	−1.3	−1.0	−1.5	−2.0	−2.0	−1.2	5.9				6.0				4.8	−0.4
100	−0.2	−1.3	−1.2	−0.9	−1.7	−2.3	−1.8	0.9	5.1			4.6	6.0				5.1	−0.2
80	0.1	−1.0	−0.9	−0.8	−1.8	−1.6				6.7	3.4	1.5	6.0				5.3	0.1
60	0.2	−0.8	−0.7	−0.6	−1.7	1.0				5.3	0.1	0.6	5.8				5.5	0.2
40	0.5	−0.6	−0.5	−0.4	−1.4	0.3					−0.4	0.0	5.5				5.8	0.5
20	2.8	0.3	0.0	0.2	−0.6	−0.9					6.8	−0.3	5.4					2.8
0		4.3	1.1	0.8	0.1	−0.7	1.8					2.4	5.0					
−20	2.4	2.6	1.2	0.5	−0.1	−0.8	−1.2	6.6					4.5				5.9	2.4
−40	−0.2	−0.9	−0.5	−0.2	−0.6	−1.0	−1.4	−1.0					5.3				4.6	−0.2
−60	−0.6	−1.2	−0.8	−0.3	−0.5	−0.8	−0.9	−0.5	4.6				5.8				4.3	−0.6
−80	−0.2	−0.9	−0.4	0.2	0.0	−0.1	0.7	3.4	6.6				3.8				4.7	−0.2
100	0.8	0.2	0.7	1.3	1.2	1.3	5.1			6.0	1.6	−0.3	4.3				5.7	0.8
−120	1.6	0.9	1.4	2.1	1.9	2.2					0.5	0.4	5.7				6.4	1.6
−140	0.8	0.1	0.6	1.2	1.0	1.2					0.9	0.2	5.4				5.8	0.8
−160	0.1	−0.8	−0.5	0.1	−0.2	−0.2	5.1				6.5	−0.2	4.8				5.1	0.1
−180	0.0	−1.0	−1.0	−0.5	−0.8	−0.9	0.4					0.9	4.7				4.9	0.0
	−180	−160	−140	−120	−100	−80	−60	−40	−20	0	20	40	60	80	100	120	120	160	180

FIGURE 13 *continued*

Part f. The lowest energy is −6.3 kcal/mol per residue, located at (−60, −40), for the infinite alanine chain *in vacuo*

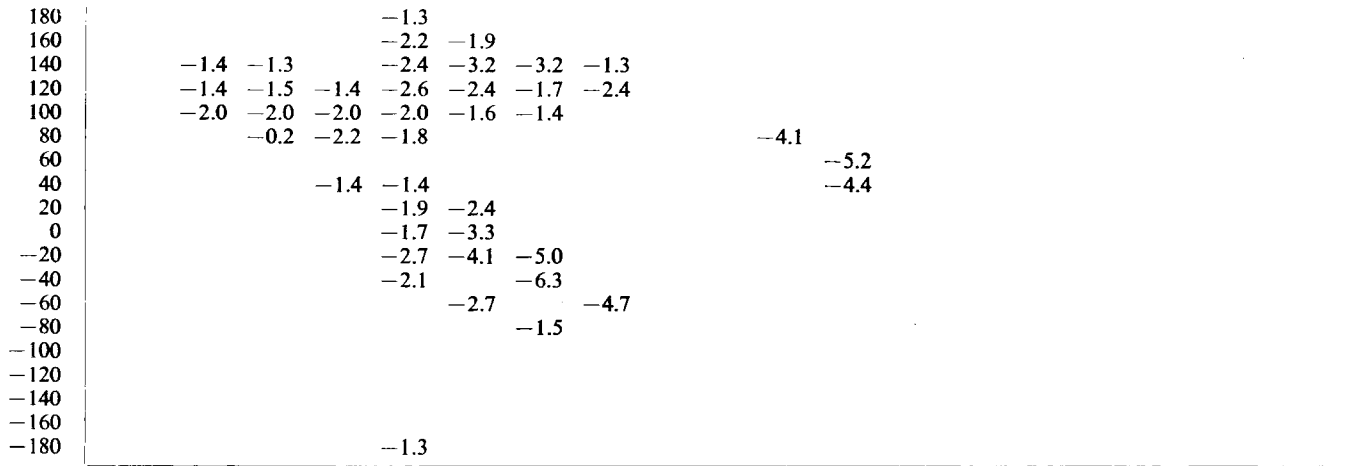

FIGURE 13 *continued*

Part g. The lowest energy is −8.2 kcal/mol per dipeptide, located at (−160,140), for the dialanine chain in water

	−180	−160	−140	−120	−100	−80	−60	−40	−20	0	20	40	60	80	100	120	140	160	180
180	−6.5	−7.8	−7.8	−7.2	−7.2	−7.0	−5.2						−3.5	−0.2			−1.6	−6.5	
160	−6.9	−8.0	−8.0	−7.5	−7.6	−7.4	−6.6	1.1					0.5	0.0			−1.8	−6.9	
140	−7.1	−8.2	−8.1	−7.6	−7.8	−7.6	−7.1	−5.2						0.5			−1.8	−7.1	
120	−6.9	−8.1	−8.0	−7.5	−7.8	−7.7	−7.2	−5.9	1.4					0.9			−1.5	−6.9	
100	−6.6	−7.8	−7.7	−7.3	−7.8	−7.9	−6.8	−3.7	0.8				0.0	1.0			−1.2	−6.6	
80	−6.3	−7.5	−7.4	−7.1	−7.8	−7.1						−0.8	−3.0	0.9			−1.0	−6.3	
60	−6.1	−7.2	−7.2	−6.9	−7.6	−4.4					1.3	−4.0	−3.8	0.8			−0.8	−6.1	
40	−5.9	−7.1	−7.0	−6.6	−7.4	−5.2						−4.4	−4.3	0.6			−0.6	−5.9	
20	−3.6	−6.3	−6.5	−6.1	−6.6	−6.4							−4.5	0.6				−3.6	
0		−2.3	−5.5	−5.6	−6.1	−6.3	−3.1						−1.8	0.3					
−20	−4.0	−4.0	−5.5	−6.0	−6.4	−6.5	−6.2							−0.2			−0.5	−4.0	
−40	−6.7	−7.6	−7.3	−6.8	−6.9	−6.8	−6.5	−5.4						0.6			−1.7	−6.7	
−60	−7.0	−7.9	−7.5	−6.8	−6.9	−6.7	−6.2	−5.1	0.6					1.3			−1.9	−7.0	
−80	−6.6	−7.5	−7.1	−6.3	−6.4	−6.1	−4.8	−1.6						−0.8			−1.6	−6.6	
−100	−5.7	−6.5	−6.0	−5.3	−5.3	−4.8	−0.6					−2.1		−0.3			−0.7	−5.7	
−120	−5.0	−5.8	−5.3	−4.5	−4.5	−3.9						−3.2		0.9			0.0	−5.0	
−140	−5.8	−6.7	−6.2	−5.4	−5.5	−4.9						−3.0	−4.0	0.5			−0.7	−5.8	
−160	−6.4	−7.6	−7.3	−6.6	−6.6	−6.3	−0.7						−4.5	−0.2			−1.4	−6.4	
−180	−6.5	−7.8	−7.8	−7.2	−7.2	−7.0	−5.2						−3.5	−0.2			−1.6	−6.5	

FIGURE 13 *continued*

Part h. The lowest energy is −5.0 kcal/mol per residue, located at (−60, −40), for the infinite alanine chain in water

	−180	−160	−140	−120	−100	−80	−60	−40	−20	0	20	40	60	80	100	120	140	160	180
180	−1.1	−1.7	−2.7	−2.2	−2.5	−0.9													−1.1
160	−1.5	−3.0	−3.0	−2.5	−3.5	−2.7	−1.3												−1.5
140	−2.8	−3.4	−3.2	−2.7	−3.7	−4.1	−2.7	−1.0										−0.2	−2.8
120	−2.7	−3.3	−3.3	−2.9	−3.8	−3.2	−2.1	−2.2											−2.7
100	−1.4	−3.7	−3.7	−3.4	−3.1	−2.4	−1.7												−1.4
80	−2.3	−1.8	−1.8	−3.5	−3.0	−1.8													−2.3
60	−1.4	−2.2	−1.5									−2.7							−1.4
40	−1.2	−2.1	−2.4	−2.6	−2.5	−0.6							−4.0						−1.2
20		−1.2	−1.8	−2.1	−2.9	−3.0							−3.8	−0.8					
0				−1.5	−2.6	−3.6	−0.9						−0.6	−0.9					
−20					−2.5	−4.0	−4.3							−0.5					
−40	−2.1	−2.3	−1.8				−5.0												−2.1
−60	−2.4	−2.6	−2.3	−1.8	−1.7			−3.6										0.0	−2.4
−80	−2.8	−3.0	−1.0	−1.4	−1.6														−2.8
−100													−0.4						
−120												−0.1							
−140													−0.8						
−160		−1.7	−2.4	−1.8	−1.9	−1.6													
−180	−1.1	−1.7	−2.7	−2.2	−2.5	−0.9													−1.1

FIGURE 13 *continued*

Part i. The lowest energy is −28.0 kcal/mol per dipeptide, located at (−80,120), for the dialanine chain in acetic acid

180	−22.9	−24.2	−23.9	−23.8	−25.1	−26.9	−23.7					−22.3	−19.7					−22.9
160	−23.0	−24.2	−23.7	−23.7	−24.9	−26.6	−25.8					−18.2	−19.6					−23.0
140	−24.4	−24.8	−24.8	−24.1	−25.4	−27.2	−27.9	−23.8					−18.9				−18.5	−24.4
120	−24.3	−25.1	−24.4	−24.0	−26.4	−28.0	−27.8	−26.7	−18.3				−19.1				−18.7	−24.3
100	−23.9	−24.6	−23.6	−23.4	−25.8	−26.5	−24.6	−21.8				−19.6						−23.9
80	−21.6	−22.4	−22.6	−22.4	−24.8	−23.7					−19.0	−21.7						−21.6
60	−22.5	−23.2	−22.4	−23.6	−24.7	−20.9					−23.1	−25.0	−18.0					−22.5
40	−21.6	−22.7	−23.0	−23.0	−23.9	−21.9					−24.1	−25.2	−19.1					−21.6
20	−18.7	−21.3	−21.2	−21.4	−23.5	−22.6						−23.6	−19.1					−18.7
0			−20.4	−20.8	−23.0	−24.0	−20.1					−20.0	−18.4					
−20	−19.4	−19.2	−20.2	−20.8	−22.5	−25.4	−24.1											−19.4
−40	−22.0	−22.6	−21.8	−21.2	−22.4	−25.2	−25.4	−23.2										−22.0
−60	−23.6	−23.2	−22.2	−21.5	−24.2	−24.5	−25.5	−22.5										−23.6
−80	−21.8	−23.0	−22.3	−21.6	−22.7	−24.3	−22.1	−18.1										−21.8
−100	−22.6	−22.6	−21.8	−22.1	−23.3	−23.0	−18.8				−20.8	−22.4	−18.3					−22.6
−120	−22.0	−23.0	−22.8	−22.1	−23.5	−23.2					−24.0	−24.0	−18.5					−22.0
−140	−22.8	−23.8	−23.0	−23.0	−24.3	−23.9					−21.5	−24.5	−18.0					−22.8
−160	−23.0	−24.4	−24.3	−23.6	−25.6	−26.5	−19.2					−24.1	−19.1					−23.0
−180	−22.9	−24.2	−23.9	−23.8	−25.1	−26.9	−23.7					−22.3	−19.7					−22.9
	−180	−160	−140	−120	−100	−80	−60	−40	−20	0	20	40	60	80	100	120	140	160	180

FIGURE 13 *continued*

Part j. The lowest energy is −7.1 kcal/mol per residue, located at (−100,120), for the infinite alanine chain in acetic acid

180	−3.0	−3.6	−4.1	−3.2	−4.1	−3.1												−3.0
160	−3.7	−4.8	−4.3	−3.5	−5.0	−4.8												−3.7
140	−5.8	−6.1	−5.3	−4.3	−5.9	−6.8	−4.6										−2.9	−5.8
120	−6.2	−6.6	−6.0	−5.0	−7.1	−6.7	−3.7										−2.5	−6.2
100	−4.5	−6.8	−6.1	−5.4	−5.8	−3.6												−4.5
80	−2.9	−2.4	−3.1	−4.5	−4.0													−2.9
60		−2.7																
40																		
20																		
0																		
−20																		
−40																		
−60																		
−80	−3.0	−2.9																−3.0
−100		−2.4	−3.0															
−120																		
−140																		
−160	−2.9	−3.5	−3.8	−3.0	−4.2													−2.9
−180	−3.0	−3.6	−4.1	−3.2	−4.1	−3.1												−3.0
	−180	−160	−140	−120	−100	−80	−60	−40	−20	0	20	40	60	80	100	120	140	160	180

FIGURE 13 *continued*

Part k. The lowest energy is −15.4 kcal/mol per dipeptide, located at (−140,100), (−180,−80), (−140,−80), for the dialanine chain in formic acid

180	−12.8	−13.0	−13.6	−12.4	−13.2	−13.7	−12.3						−10.6	−6.6				−7.4	−12 8
160	−12.9	−12.9	−13.3	−12.1	−12.8	−13.0	−14.5						−5.8	−7.0				−7.5	−12.9
140	−13.8	−13.7	−13.9	−12.6	−13.2	−13.3	−14.6	−12.7						−7.8				−8.2	−13.8
120	−14.8	−13.6	−13.8	−13.4	−13.1	−13.7	−15.1	−13.9	−5.3					−7.5				−8.9	−14.8
100	−15.0	−15.0	−15.4	−14.0	−14.3	−14.6	−13.7	−10.8	−7.9				−8.9	−7.8				−9.2	−15.0
80	−14.6	−14.6	−14.8	−13.9	−14.0	−13.8						−8.5	−11.6	−7.2				−9.0	−14.6
60	−12.9	−13.0	−14.4	−13.7	−14.1	−10.6					−5.7	−13.6	−13.0	−6.4				−7.2	−12.9
40	−11.2	−11.4	−12.0	−12.4	−11.8	−9.3						−11.9	−8.4	−5.4				−5.4	−11.2
20	−9.3	−10.9	−11.8	−11.2	−12.1	−11.6								−6.7					−9.3
0		−6.8	−10.6	−10.3	−11.9	−12.3	−7.8							−7.0					
−20	−9.6	−8.5	−10.5	−10.4	−10.5	−12.2	−13.1	−9.4						−6.6				−5.7	−9.6
−40	−12.5	−12.2	−12.4	−11.2	−11.0	−12.0	−13.3	−11.9										−7.1	−12.5
−60	−14.6	−14.4	−14.5	−13.2	−13.8	−13.7	−14.3	−14.1	−6.0					−6.4				−9.1	−14.6
−80	−15.4	−15.3	−15.4	−14.0	−13.6	−13.8	−12.3	−8.4						−8.7				−9.7	−15.4
−100	−14.0	−13.9	−14.0	−12.6	−12.5	−13.0	−8.3				−6.1	−8.8	−11.7	−7.4				−8.5	−14.0
−120	−12.9	−12.6	−12.6	−11.3	−11.3	−12.0						−10.7	−12.0	−5.3				−6.2	−12.9
−140	−12.5	−12.6	−13.8	−12.3	−12.3	−13.2						−9.6	−11.6					−6.8	−12.5
−160	−12.4	−12.6	−13.0	−12.8	−12.6	−13.4	−6.8						−12.1	−5.4				−6.7	−12.4
−180	−12.8	−13.0	−13.6	−12.4	−13.2	−13.7	−12.3						−10.6	−6.6				−7.4	−12.8
	−180	−160	−140	−120	−100	−80	−60	−40	−20	0	20	40	60	80	100	120	140	160	180

FIGURE 13 *continued*

Part 1. The lowest energy is 5.0 kcal/mol per residue, located at (−60, −40), for the infinite alanine chain in formic acid

	−180	−160	−140	−120	−100	−80	−60	−40	−20	0	20	40	60	80	100	120	140	160	180
180			−0.7	−0.6	−1.1														
160		−0.6	−0.8	−0.7	−1.9	−1.7													−1.0
140	−1.0	−1.0	−1.0	−0.8	−2.0	−2.9	−1.4	−0.5											−2.1
120	−2.1	−1.2	−1.3	−1.1	−2.2	−2.1	−0.5	−1.3											−0.2
100	−0.2	−2.1	−1.8	−1.1	−0.8	−0.6	−0.4												−0.7
80	−0.7			−1.0	−0.8						−1.3								
60		−0.3											−4.4						
40		−0.3	−0.3	−1.2	−1.1								−3.1	−0.4					
20					−1.5	−2.4							−0.6						
0					−1.1	−2.7	−0.9												
−20					−1.8	−3.5	−4.6												−0.7
−40	−0.7	−0.3					−5.0												0.0
−60	0.0							−1.6											
−80																			
−100																			
−120													−0.4						
−140																			
−160			−0.5	−0.2	−0.4	−0.3													
−180			−0.7	−0.6	−1.1														

FIGURE 13 *continued*

approximately the same stabilization polymer-solvent interaction energy with the dipeptide of L-alanine as these two less polar solvents. L-alanine oligomers have more favorable interactions with aqueous solution than with methanol and ethanol as the length of the chain increases.

The energy maps of LCA in methanol and ethanol are nearly identical. The right-handed α helix, located near $\phi = -60°$, $\psi = -40°$, is the preferred conformation for both solvents. Relative minima at $\phi = -160°$, $\psi = 100°$ and $\phi = -80°$, $\psi = 140°$, on both maps, are indicative of the possible existence of isolated stable β- and left-handed 3_1-helical conformations, respectively. For ethanol, in fact, the right-handed α helix and the left-handed 3_1 helix are approximately equally stable.

The conformational energy map of LCA in vacuum contains more significant variations in energy than the methanol and ethanol maps. This suggests that LCA in vacuum can adopt fewer conformational states than in methanol and ethanol. This map indicates less flexibility of the biopolymer than computed by other workers.[70] The reason for this is due to an increase in the stabilization energy given to the hydrogen bond. In these calculations the ΔH of breaking the hydrogen bond of the α helix in water is 1.5 kcal/mol.[71] This requires a pairwise intrachain hydrogen bonding energy of -4.6 kcal/mol, as compared to the -3.5 kcal/mol normally used. These calculations indicate that in this case LCA in vacuum would prefer the right-handed α-helical conformation.

LCA in aqueous solution also is most stable as a right-handed α helix. However, the conformational flexibility of the polymer is much enhanced over what it was in vacuum. There are relative minima located at points on the map corresponding to β- and left-handed 3_1-helical structures just as for methanol and ethanol.

The conformational map of LCA in acetic acid indicates a radical departure in the conformational properties of the biopolymer. Only conformations in the upper left-hand corner of the map, β- and left-handed 3_1-helical type structures, are permitted. The global minimum is at $\phi = -100°$, $\psi = 120°$. A relative minimum is also noted near the β position on the map. This radical change in the conformational properties is not too surprising since one expects the polar groups of the solvent molecules to strongly interact with LCA. Interactions involving the carbonyl oxygen and amide hydrogen with solvent would be especially stabilizing.[54] The net effect of such interactions would be to "pull" the α helix apart in order to expose the carbonyl oxygens and amide hydrogens in solvent. Thus extended structures should be preferred.

An extended structure, a near left-handed 3_1 helix, presently called the *extended coil*, has been identified for the charged form of poly(L-glutamic acid) in aqueous solution.[72] This conformation is mainly stabilized by the interaction of the COO^- groups with solvent, and the minimizing of the intrachain electrostatic energy by maximizing the distance between COO^- groups. Solvent

interactions with backbone carbonyl and amide groups make favorable contributions to the promotion of the extended coil, but are small in comparison to the interactions involving COO^- groups. This new conformation was discovered, in part, because its CD/ORD spectra are similar to poly-(L-proline) II spectra. Recently, a number of workers studying more exotic polymer-solvent systems have reported CD spectra similar to that of poly-(L-proline) II. A list of these studies is given in Ref. 73; several examples are $[N^5$–(2-hydroxy-ethyl)–L-glutamine$]_n$ in water,[74,75] (γ–ethyl-L-glutamate)$_n$ in sulfuric acid–water mixtures,[76] (γ–methyl-L-glutamate)$_n$ in fluor gem-dials,[73] and (phenylalanine)$_n$ in methane sulfonic acid–water mixtures.[77] If these polymers adopt the extended coil conformation it cannot be stabilized by the strong electrostatic repulsions present in poly(L-glutamic acid). In view of the calculations reported here, such structures are stable due to highly favorable interactions between carbonyl oxygens and/or amide hydrogens in the peptide backbone with the highly polar solvent molecules.

However, the conformational map of LCA in formic acid contradicts the conclusion of the preceding paragraph. The first thought one should have is to expect LCA in formic acid to behave nearly the same as in acetic acid. An inspection of the map of LCA in formic acid indicates that the biopolymer has conformational properties very similar to LCA in aqueous solution. From an inspection of the polymer-solvent parameters presented in Table VII it is seen that the Δf's of formic acid and acetic acid are nearly identical while the R_v's of formic acid are about midway between the R_v's of water and acetic acid. The first five and the seventh V_f listed in Table VII are necessary to describe interactions between solvent and poly(L-alanine). In four out of six of these cases the V_f for formic acid are closer in value to the V_f of water than that of acetic acid. This includes the important carbonyl oxygen and amide hydrogen values.

It is concluded from these observations that in this case the size and shape of the solvent molecule overrides the free energy interactions between solvent and solute species in specifying conformation. This is a consequence of the model; whether or not such a volume effect due to size and topology of solvent molecules can be such a critical factor in dictating conformation is not known.

Note that chain-aggregation, or chain folding, which could provide stabilization free energy through inter- or intra-chain hydrogen bond formation, respectively, is not taken into consideration in these calculations. The extent of polymer-solvent interactions could also be seriously modified by chain-aggregation, or chain-folding, through excluded volume effects. This discussion is valid only for isolated chains of L-alanine which presumably corresponds to very dilute solutions.

Figure 14 demonstrates how the mean square residue-length, $\langle \hat{l}_k^2 \rangle$, of an

L-alanine unit depends upon solvent and ordered chain-length. Two general observations can be made from Figure 14; first, all five solvents promote the unfolding of the right-handed α helix, and, secondly, the ordered secondary structures for k > 14, *i.e.*, chains longer than fourteen residues, have $\langle \hat{l}_k^2 \rangle$ values nearly identical to the polymer. This suggests that L-alanine oligomers composed of fourteen or more residues are very nearly identical to the polymer in ordered secondary structure in all five solvents considered here.

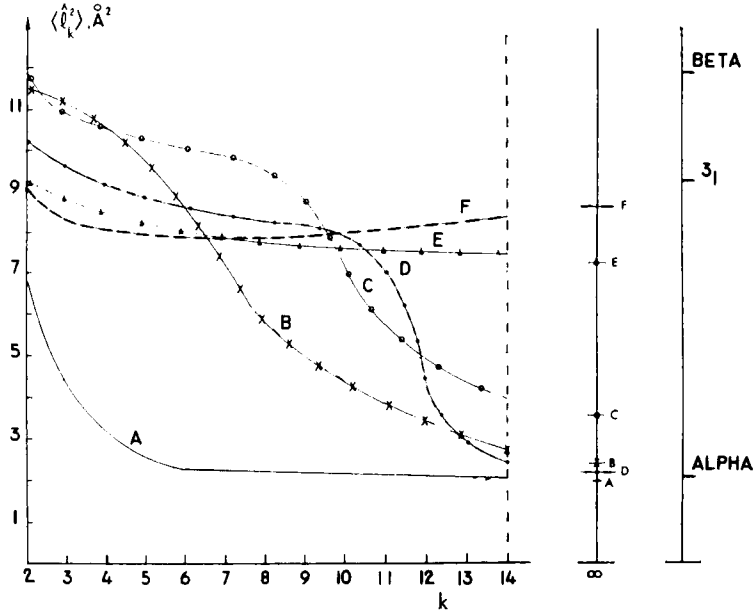

FIGURE 14 Plots of $\langle \hat{l}_k^2 \rangle$ *vs.* k for ordered chains of L-alanine in five sovents and *in vacuo*. The values of $\langle \hat{l}_k^2 \rangle$ for various standard secondary structures and for $k \rightarrow \infty$ are shown at the right in the figure. (A) *in vacuo*, (B) methanol, (C) water, (D) formic acid, (E) ethanol, (F) acetic acid. Reprinted from Ref. (134) by courtesy of the American Chemical Society.

Oligomeric L-alanine chains in vacuum, water, methanol and formic acid undergo an extended conformation → right-handed α helix transition as a function of increasing k. At some specific chain length, different for each solvent, the energy gained by the formation of the intrachain hydrogen bonds overcomes the stabilization energy resulting from the polymer-solvent interactions. For acetic acid the polymer-solvent interaction energy stabilizes extended secondary structures to such a degree than an α helix is not realized. In ethanol there is a balanced equilibrium between the formation of α helix and the retention of extended conformations leading overall to a large value for $\langle \hat{l}_k^2 \rangle$.

Trans-proline

In Figure 15 are shown the conformational energy maps, using the notation of Krimm and Venkatachalam,[59] for two peptide units of *trans*-L-proline, and for a long ordered chain of *trans*-L-proline peptide units (LCTP). The former is the model for the least-ordered, or random, form of *trans* poly(L-proline) (RCTP), and the latter is a model for the perfectly ordered polymer. Figure 15 contains conformational energy maps for each of the five solvents discussed in this section. Figure 10 contains the *cis*- and *trans*-poly(L-proline) energy maps computed by Krimm and Venkatachalam.[59]

RCTP has two major energy minima. The deepest and broadest lies in the region $\psi = 120°$ to 180°, and $\omega = 160°$ to 200°. This minimum corresponds to the left-handed 3_1 helix observed in the solid state.[78] The other minimum occurs in the region of the right-handed α helix, $\psi = -60°$. This particular conformation has been observed for proline residues in several globular proteins.[79] There is, at present, considerable debate whether this minimum is possible for a dimer of *trans*-L-proline. Some workers feel it is an artifact of inaccurate potential functions. RCTP is very sensitive to solvent in the sense that the magnitude of the polymer-solvent interaction varies considerably with the choice of solvent. The stable secondary structures of RCTP, however, are rather insensitive to solvent. Both methanol and ethanol have a greater stabilizing interaction with RCTP than water. The reason for this is due to the absence of the NH group and the addition of the CH_2 groups from the pyrrolidine ring. The only highly favorable interaction of the water molecules with the proline residue is through the carbonyl oxygen. However, some of the stabilization free energy gained through this interaction is lost to unfavorable interactions between the water molecules and the ring CH_2 groups. Methanol and ethanol, on the other hand, have a moderately favorable interaction with the carbonyl oxygen, through the OH group, and with the CH_2 units, through hydrophobic bonding with the CH_3 or CH_2CH_3 groups of methanol or ethanol, respectively. Thus it appears that these two moderately favorable interactions of methanol and ethanol with RCTP are more stabilizing than the difference between one highly stabilizing and several slightly destabilizing interactions as takes place when water molecules interact with RCTP. The absence of the NH group prevents a water molecule from acting as a binary-binding solvent species. The interaction of the carbonyl oxygen of RCTP with the neutral forms of acetic and formic acids is sufficiently stabilizing so that both these solvents interact more favorably with RCTP than the other three solvents considered here.

In all solvents torsional rotations about the imide bond up to $\pm 10°$ are energetically possible. The global minima, however, always occur for $\omega = 180°$. The shape of the minima, specifically their broadness with respect to ω, suggests fluctuations in ω occur at room temperature in all five solvents.

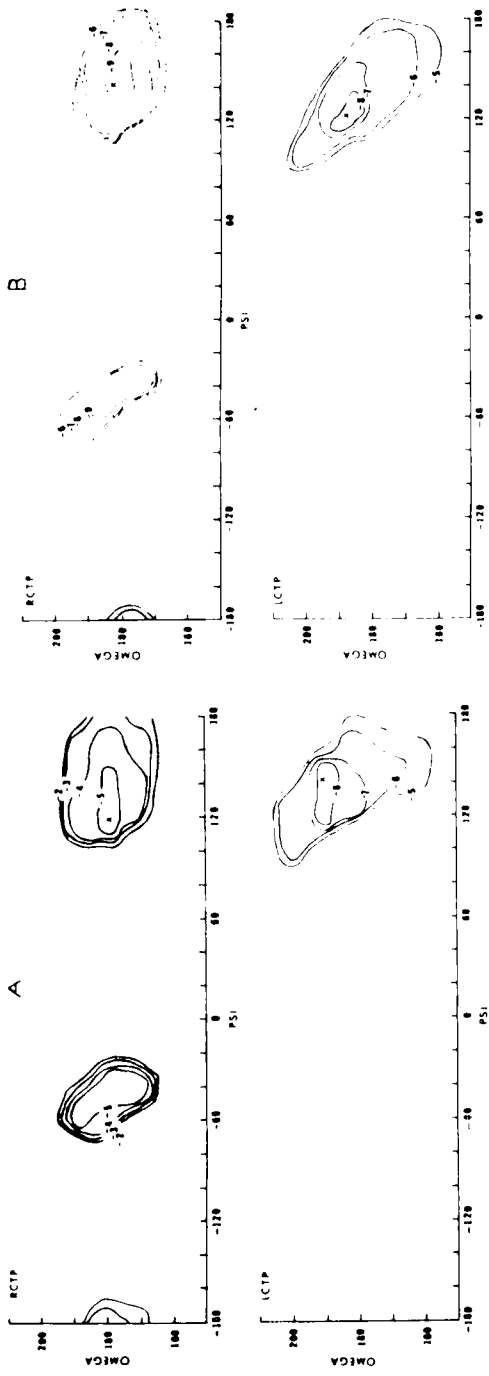

FIGURE 15 Conformational energy maps of ω (rotation about the C′-N imide bond) *vs.* ψ for RCTP and LCTP. The torsional rotation barrier about the C′-N is $V(\omega) = \frac{1}{2} V_0 (1 - \cos 2\omega)$ with $V_0 \approx 20$ kcal/mol.[67] The energy contours are in kcal/mol of residue. The $\times$ denote the global minima. (A) *in vacuo*, (B) aqueous solution, (C) methanol, (D) ethanol, (E) formic acid, (F) acetic acid. Reprinted from Ref. (134) by courtesy of the American Chemical Society.

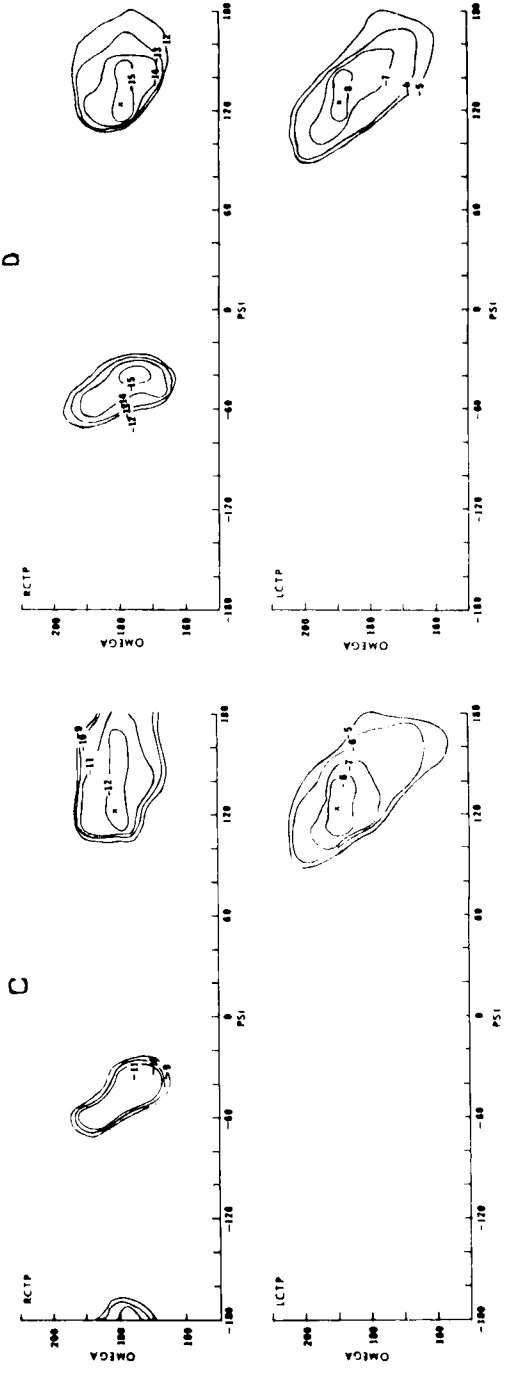

FIGURE 15 *continued*

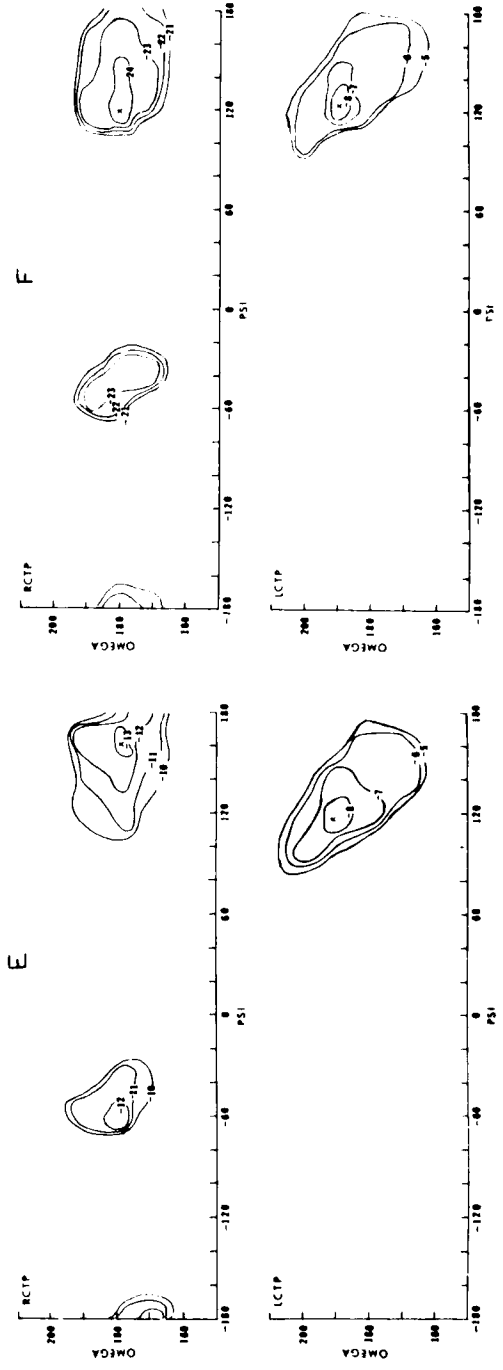

FIGURE 15 *continued*

The conformational energy maps of LCTP possess a single minimum in conformational energy which corresponds to the left-handed 3_1 helix. Each of the five solvents interact with LCTP in such a way that the total resultant polymer-solvent interaction is small. In each instance, the stereochemistry of the left-handed 3_1 helix is apparently sufficiently restrictive to preferential solvent binding so that the stabilization free energy, realized through carbonyl oxygen–polar group of the solvent molecule interaction plus either favorable, or unfavorable, CH_2-solvent molecule interactions, results in total interaction free energies between LCTP and solvent which are only slightly stabilizing. At first this would appear contrary to the findings of Krimm and Venkatachalam[59] who conclude that LCTP is very much stabilized as a left-handed 3_1 helix through interactions with water. However, the findings in the two studies are identical if *only* the interactions of water molecules with the carbonyl oxygens are considered here as done in the Krimm-Venkatachalam calculations. Nevertheless, there is a substantial decrease in stabilization free energy when the remainder of the LCTP atoms are allowed to interact with water. The $CH_2 \ldots H_2O$ polymer-solvent interactions are the primary source of the destabilization free energy.

Torsional rotations about the imide bond up to $\pm 10°$ may occur in LCTP. The global minimum, for all solvents, occurs at $\omega \approx 187°$. This is the first instance in which a non-planar configuration of a peptide unit has been shown to be energetically more favorable than the corresponding planar geometry.

In Figure 16 is a plot of $\langle \hat{l}_k^2 \rangle$ versus k for *trans*-L-proline molecules in the five solvents and vacuum. An analysis of this plot indicates that only the small, $k < 4$, oligomers of *trans*-L-proline are conformationally sensitive to solvent. Further, only these small oligomers have the capacity to adopt secondary structures other than the left-handed 3_1 helix. The low energy region near $\psi = -60°$, $\omega = 180°$ provides this added chain flexibility up to $k = 4$. For *trans*-L-proline oligomers consisting of four or more peptide residues the left-handed 3_1 helix is the preferred secondary structure of LCTP in all five solvents and vacuum. These findings are in agreement with earlier experimental studies[80] where, in aqueous solution, the left-handed 3_1 helix was preferentially adopted starting with the tetra(*trans*-L-proline) oligomer.

Cis-proline

Figure 17 contains conformational energy maps of RCCP, random chain *cis*-L-proline, and LCCP, long chain *cis*-L-proline, in vacuum and aqueous solution. The RCCP maps contain two minimum energy regions. The deepest, in the vicinity of $\omega = 0°$ and $\psi = 160°$, corresponds to the secondary structure observed in the solid state.[81] The second minimum corresponds to a conformation in which the second planar peptide unit lies in plane which nearly bisects

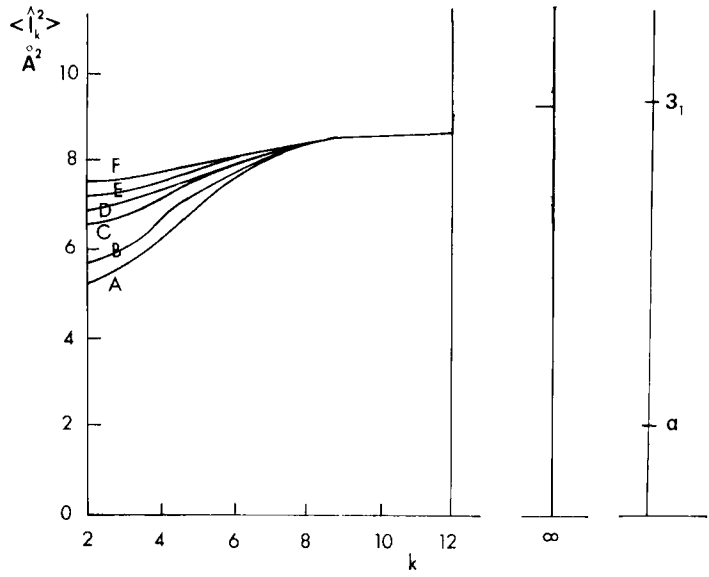

FIGURE 16 Plots of $\langle \hat{l}_k^2 \rangle$ *vs.* k for ordered chains of *trans*-L-proline in five solvents and *in vacuo*. The values of $\langle \hat{l}_k^2 \rangle$ for two standard secondary structures and for $k \rightarrow \infty$ are shown at the right in the figure. (A) methanol, (B) *in vacuo*, (C) water, (D) formic acid, (E) ethanol, (F) acetic acid. Reprinted from Ref. (134) by courtesy of the American Chemical Society.

the N—C^{α}—C^{β} bond angle of the pyrrolidine ring of the first planar peptide unit. The carbonyl oxygen bond of the second residue is pointed away from the pyrrolidine ring of the first residue. RCCP shows about the same conformational sensitivity to solvent as does RCTP. This is demonstrated in the Figure 18 where $\langle \hat{l}_k^2 \rangle$ of *cis*-L-proline is plotted as a function of k, the number of residue units in an ordered chain. The maximum variation in $\langle \hat{l}_k^2 \rangle$ as a function of solvent takes place for $k = 2$.

The conformational properties of LCCP are extremely insensitive to solvent. The severe stereochemical restrictions in this biopolymer, as reflected in the vacuum and aqueous solution conformational energy maps, do not allow polymer-solvent interactions to modify secondary chain structure. In Table IX are listed the values of the polymer-solvent interactions of LCTP and LCCP for each of the respective global energy minima. It is noted that the interactions of LCCP with solvent are smaller in magnitude than the corresponding polymer-solvent interactions of LCTP. This is in qualitative agreement with the findings of Krimm and Venkatachalam.[59] Also, the *cis* form of the biopolymer exhibits a less polar, more hydrophobic character in the polar solvents than does the *trans* form. This finding is in agreement with experiment.[60] The enhanced hydrophobic character of the *cis* form is due to, as postulated,[60]

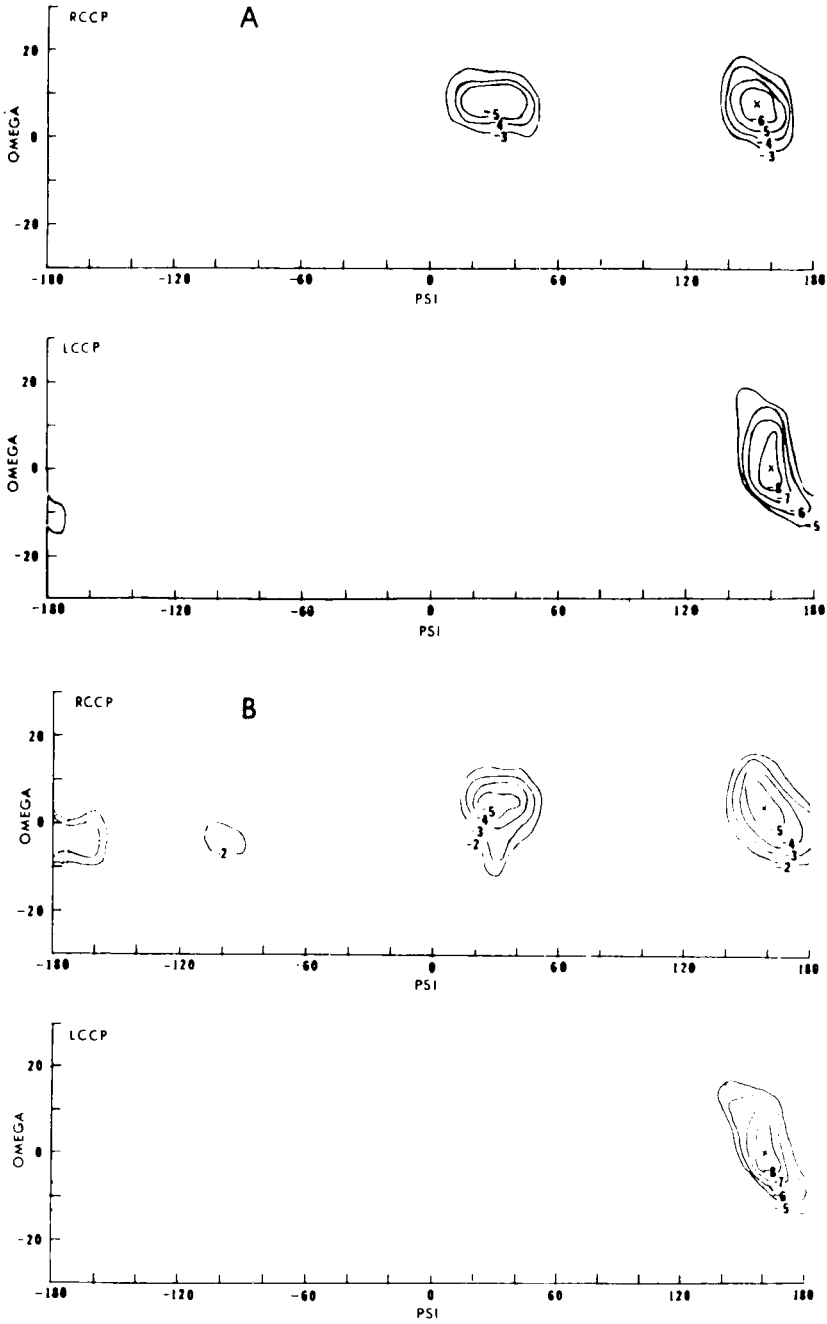

FIGURE 17 Conformational energy maps of ω *vs.* ψ for RCCP and LCCP (A) *in vacuo*, (B) aqueous solution. The energy contours are in kcal/mol of residue and $\times$ denotes global minimum. Reprinted from Ref. (134) by courtesy of the American Chemical Society.

greater exposure of the pyrrolidine rings to solvent, and less exposure of the carbonyl oxygens. Values of $|\omega| \leq 10°$ are possible for both RCCP and LCCP with the energy minima always occurring at $\omega = 0°$.

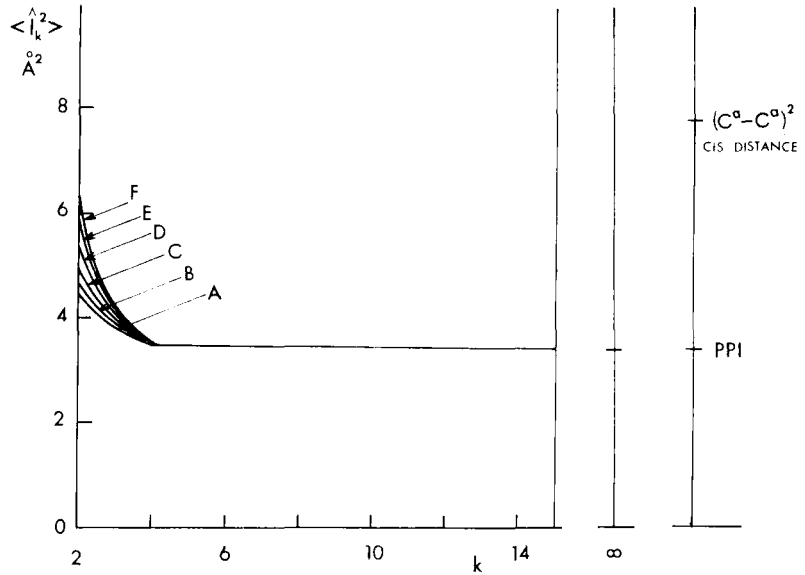

FIGURE 18 Plots of $\langle \hat{l}_k^2 \rangle$ *vs.* k for ordered chains of *cis*-L-proline in five solvents and *in vacuo*. The values of $\langle \hat{l}_k^2 \rangle$ for the polymeric form in the solid state, PP I, is listed at the far right along with the $(C^{\alpha} - C^{\alpha})^2$ distance of the *cis*-residue for $\omega = 0°$. (A) *in vacuo*, (B) methanol, (C) formic acid, (D) water, (E) ethanol, (F) acetic acid. Reprinted from Ref. (134) by courtesy of the American Chemical Society.

TABLE IX

Characteristic polymer-solvent interactions of LCTP and LCCP[a]

Solvent	LCTP	LCCP
Water	−0.5	+0.1
Methanol	−0.2	+0.2
Ethanol	−0.6	0.0
Formic acid	−0.4	−0.1
Acetic acid	−0.8	−0.3

[a]See text for definitions. These values were obtained at the global minima in total conformational energy. Energies are in kcal/mol of residue.

Reprinted from Ref. (134) by courtesy of the American Chemical Society.

4 SOLVENT-DEPENDENT CONFORMATIONAL STUDIES OF THE S-PEPTIDE OF RIBONUCLEASE-S

The denaturation of proteins by solvent media is a classic phenomenon in protein chemistry. Unfortunately, the molecular thermodynamics of the unfolding of polypeptide chains is not well understood. One way of studying protein denaturation on the molecular level is to carry out solvent-dependent conformational energy calculations on a "small" hetero-sequenced polypeptide chain which has the capacity to unfold. The S-peptide of ribonuclease-S,[82] which consists of the first twenty amino acid residues from the N-terminal end of the protein,

H – Lys – Glu – Thr – Ala – Ala – Ala – Lys – Phe – Glu – Arg –
(1) (2) (3) (4) (5) (6) (7) (8) (9) (10)

Gln – His – Met – Asp – Ser – Ser – Thr – Ser – Ala – Ala – OH
(11) (12) (13) (14) (15) (16) (17) (18) (19) (20)

can unfold from the initial tertiary structure it possesses when near the parent protein to some different tertiary structure which depends upon the solvent medium. Since the X-ray structure of the parent protein and S-peptide are known[82] when the two are complexed there is an initial starting point in the conformational energy minimization which greatly facilitates the computations.

Solvent-dependent conformational energy calculations, using the hydration shell model discussed above, of the S-peptide have been carried out in water, formic acid, and acetic acid. The polar side chains were taken to be in the charged state. A Monte Carlo minimization technique, described elsewhere,[65] in which one *assumes* to be at a minimum when no change in the most stable conformational energy occurs for a large number of random perturbations of the internal bond rotation angles was used in the structural refinements. The maximum absolute values of the random perturbations of the bond rotation angles were 10° for ϕ and ψ, 5° for ω, and 15° for the χ in all calculations. The Davidon minimization scheme,[62] which is perhaps the most promising technique to minimize a function of many variables, still was operationally too slow to be of practical use in this investigation.

Two major observations were made after carrying out the solvent-dependent conformational energy calculations on the S-peptide:

a) No significant changes in conformation took place during the Monte Carlo minimizations regardless of the choice of solvent and/or choice of starting structure. In other words, the starting structure and final refined structure were always very similar in conformation. There are at least three ways of explaining this finding: (1) An insufficient number of random fluctuations were allowed. Thus the molecule which might have been leaving one

relative minimum region for another was stopped before reaching the new minimum region. (2) Each starting conformation was very near a relative minimum so that each minimization calculation homed-in on the nearby relative minimum resulting in a small net change in the conformation. (3) The low energy paths out of one relative minimum and into another are very complex requiring very specific interrelationships between the magnitudes and directions of the fluctuations in the bond rotation angles. The required interrelationships would be very difficult to achieve using random fluctuations. Thus, significant conformational changes did not occur in the calculations. Some type of highly specific coupling between rotational fluctuations, perhaps of a co-operative nature, may be essential to completing the conformational transition.

b) The X-ray tertiary structure of the S-peptide is not the global minimum in energy in any media tested. Major improvements in both the intrachain and solvation energies were realized by extending the polar side chains out into solvent, and moving the nonpolar side chains away from polar groups on the polar side chains. The energy was much more sensitive to changes in the conformation of the side chains than in the backbone. However, an essentially extended backbone conformation with extended side chains gave the lowest total energy for the S-peptide in acetic acid for any of the structures tested.

The energies associated with the various refined structures of the S-peptide are listed in Table X. Figure 19 contains ORTEP[83] drawings of the backbone

TABLE X

Energies of refined conformations of the S-peptide in various solvents

Conformation	Chain energy kcal/mol	Solvation energy kcal/mol	Total energy kcal/mol
X-ray	high	− 73.4	high
Side chains folded as in X-ray structure			
water	−13.0	−175.2	−188.2
acetic acid	−13.0	134.2	−147.3
Side chains extended out into solvent			
water	−51.0	−196.3	−247.3
formic acid	−51.0	82.7	−133.7
acetic acid	−51.0	−230.5	281.5
vacuum	−61.0		61.0
Extended backbone and side chains			
acetic acid	47.1	285.7	−332.8

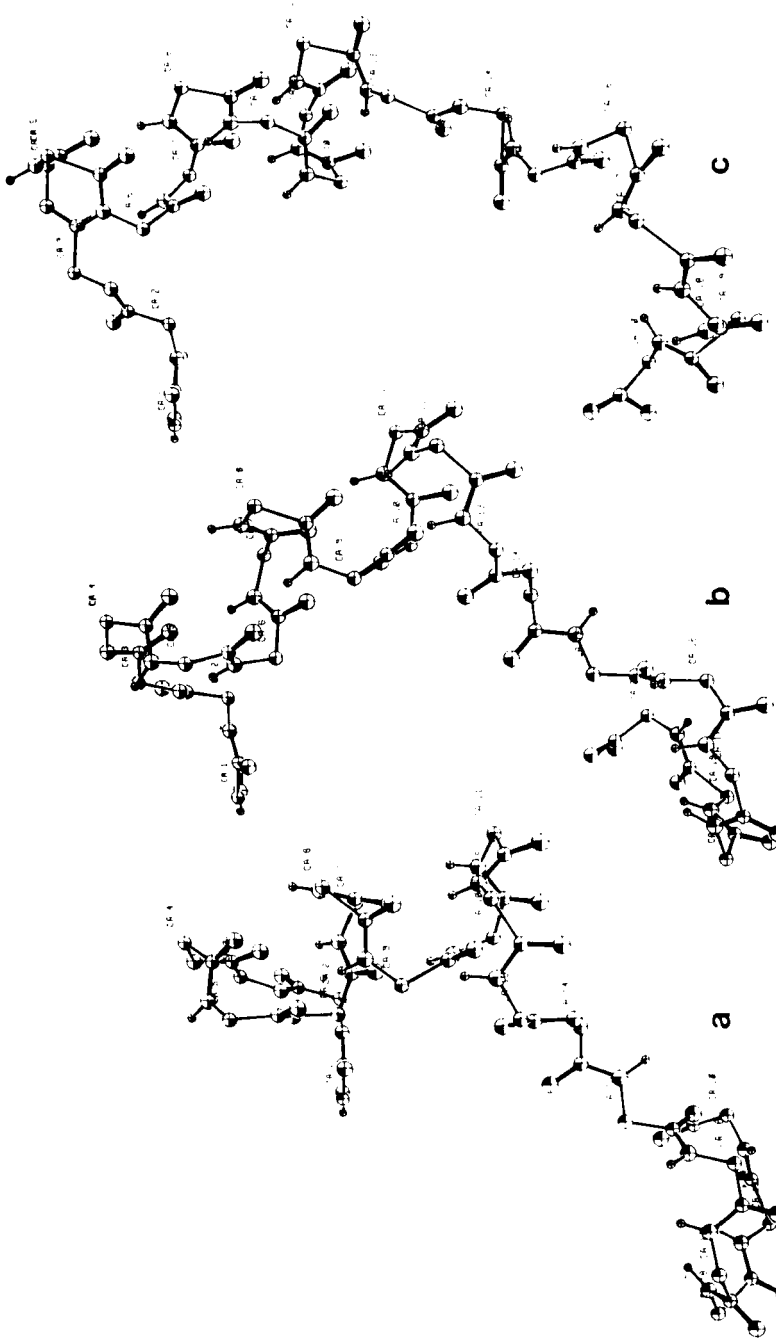

FIGURE 19 ORTEP drawings of the backbone conformation of the S-peptide for (*a*) the refined structure in water with the side chains folded, (*b*) the refined structure in formic acid with the side chains extended, (*c*) the X-ray structure.

of the S-peptide, (a) in aqueous solvent, (b) in formic acid, and (c) the X-ray structure.

These calculations roughly tend to agree with the work of Klee[84a] who concluded that the isolated S-peptide in aqueous solution often adopts, as it undergoes fluctuations, a conformation rather similar to that which it has when near the parent protein. We have found that the most stable conformation of the S-peptide in aqueous solvent has a backbone conformation nearly identical to the X-ray structure, but with side chains extended away from the backbone. Brown and Klee[84b] noted that the S-peptide denatures, becomes structureless, with the addition of strongly polar solvent components to the aqueous solution. This is at least in conceptual agreement with the finding reported here in which the destruction of the α-helical segment in favor of an extended backbone formation leads to a lower total energy in acetic acid than when the α-helical segment is maintained.

5 RELATED STUDIES

A number of studies not directly concerned with the structural geometry and/or molecular thermodynamics of polymer-solvent interactions have provided additional information about the solvation process. In this section we summarize the results of several such investigations.

Recently three papers have appeared in *Biopolymers* dealing with the conformational properties of poly(L-alanine) (PLA) in solution. In the first of these papers Brumberger and Anderson[85] determined the radius of gyration and persistence length of poly(L-alanine) in dichloroacetic acid (DCA) and a 1:1 v/v mixture of trifluoroacetic acid and trifluoroethanol (TFA:TFE) using small angle X-ray scattering. Table XI summarizes the results of their study.

TABLE XI

Radius of gyration and persistence length of poly(L-alanine) in solution

Solvent	R_G(Å)	P_L(Å)
DCA	56	44
TFA:TFE	78	≈30

The authors conclude that PLA exists in a relatively rigid, predominantly α-helical conformation in DCA and in an extended, more flexible form in TFA:TFE. It is also interesting to compare these results to those for the corresponding solid states.[86,87] From DCA, the authors found that a dendritic mat was crystallized which showed amide I and II bands in the infrared

spectrum at 1650 cm^{-1} and 1550 cm^{-1}. The spherulitic structures cast from TFA:TFE showed shifts to lower wave numbers; a shoulder developed at 1635 cm^{-1}, and barely resolved bands were observed at 1540 and 1525 cm^{-1}. Thus the material crystallized from DCA was assigned a predominantly α conformation; the TFA:TFE material appeared to possess a surface layer of α-helical PLA while the bulk of the interior was in a different, probably extended form.[86–90] Brumberger and Anderson conclude, therefore, that the solution conformation of PLA is retained at least to some degree on crystallization from these two solvent systems.

Nakajima and Murakami[91] also studied the chain conformation of poly(L-alanine) in DCA. They used a combination of experimental techniques which included optical rotatory dispersion, intrinsic viscosity and sedimentation equilibria. The characteristic ratios $\langle R_0^2 \rangle / nl^2$ obtained from the sedimentation-equilibria data are in the range 5.3–5.6, depending on the value assumed for M_z in the evaluation of sedimentation data. These values are much smaller than the 8.6 reported for "random coil" polypeptides.[92] Theoretical expressions for interrupted helices derived by Nagai,[93] and others[94–96] suggest that the characteristic ratio first decreases with increasing helical content, passes through a minimum, and then increases under appropriate conditions. In other words, the characteristic ratio of an interrupted helix is smaller than that of the perfect random coil. The result, $\langle R_0^2 \rangle / nl^2 = 5.3$–5.6, suggests therefore to Nakajima and Murakami that PLA chains assume the form of interrupted helix in DCA at 25°C. Such a conclusion is also supported by their ORD data which suggest that the helical content of the sample is about 50%.

There appears to be a discrepancy between the Brumberger and Anderson study of PLA in DCA and that of Nakajima and Murakami. The former suggests a rigid-integral α-helical conformation while the latter proposes an interrupted series of α-helical segments along the chain. While this writer is the first to admit that an exhaustive number of investigations have already been carried out on poly(L-alanine) it still would be desirable to carry out an investigation to resolve these solution-structure discrepancies. If we cannot understand the conformational properties of a simple homopolymer like poly(L-alanine) in solution how can we ever hope to understand the solution-structure properties of globular proteins!

In the final study dealing with the solution conformation of PLA, Parrish and Blout[97] found that high-molecular weight PLA dissolved in hexafluoroisopropanol possess ultraviolet, optical rotatory dispersion, circular dichroism, and infrared spectra which were not identifiable with the spectra of random chain poly(γ-morpholinylethyl-L-glutam-amide) nor with α-helical poly(γ-methyl-L-glutamate), poly(L-homoserine), poly(L-methionine), or poly(ϵ,*N*-carbobenzoxy-L-lysine) in this solvent.[98] Additionally, the PLA spectra did not coincide with those of β structures[99–104] or with mixtures of α helix,

random-chain, and β structure spectra. On the other hand, a film of PLA formed by the evaporation of the hexafluoroisopropanol solution showed a normal α helix infrared spectrum. Thus, the unique conformation of PLA in hexafluoroisopropanol could be studied only in the solution state. Using the spectroscopic tools of infrared absorption, ultraviolet absorption, circular dichroism, and optical rotatory dispersion, Parrish and Blout give considerable evidence for the existence of a new helical conformation for PLA in this strongly hydrogen bonding solvent. Figure 20 contains the ultraviolet, infrared, circular dichroism and optical rotatory dispersion spectra of PLA in hexafluoroisopropanol. Strong evidence that a helical conformation is present is shown by the high degree of hypochromism in the 187 mμ absorption peak and by the positions of the amide infrared bands. The CD and ORD spectra are also similar to those of α-helical polypeptides, though important qualitative and quantitative differences are observed. The authors suggest a new type of α helix conformation in order to explain the novel spectra, which are not mixtures of the spectra of previously reported polypeptide conformations. The postulated conformation (a doubly hydrogen-bonded helix) is a distorted α helix in which the peptide carbonyl groups point slightly out from the helix axis and are hydrogen bonded simultaneously both to the NH of the fourth

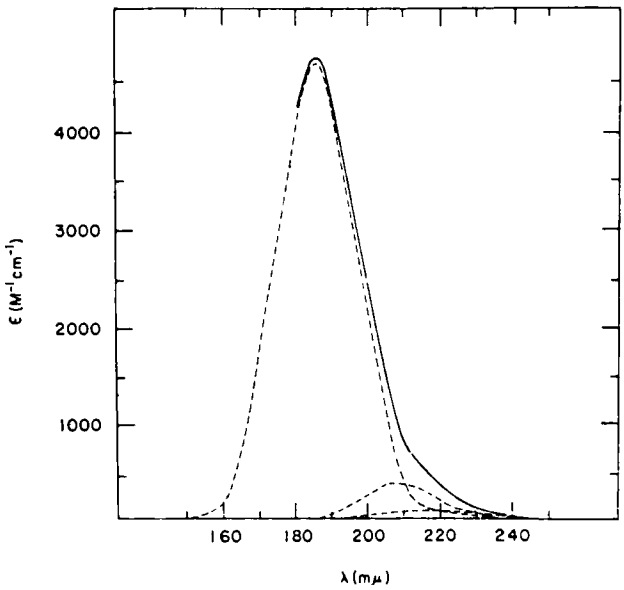

FIGURE 20(a) The resolved UV spectrum of poly(L-alanine) in hexafluoroisopropanol. (----) resolved spectral components; (————) observed spectrum. Reprinted from Ref. (97) by courtesy of John Wiley & Sons, Inc.

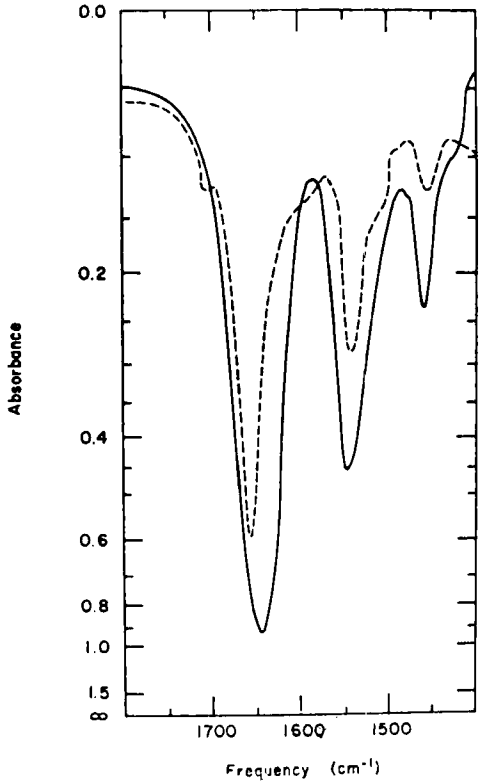

FIGURE 20(b) Infrared spectra in amide I and II regions of poly(L-alanine) as a dry film (----) and as a 4.0% solution (———) in hexafluoroisopropanol (0.05 mm CaF_2 cell). Reprinted from Ref. (97) by courtesy of John Wiley & Sons, Inc.

peptide residue to the carboxyl terminal side (as in the classical α helix), as well as to a solvent molecule's hydroxyl hydrogen.

Another series of papers which have recently appeared in the literature deal with solution thermodynamics of nucleic acid bases. In order to examine the thermodynamic effects of exposing nucleic acid bases to water, Scruggs, Achter and Ross[105] measured the solubility of adenine, cytosine and uracil in water and in organic solvents as a function of temperature.

The free energy, enthalpy, and entropy of solution in a given solvent were obtained using the familiar equations:

$$\Delta G = -RT \ln x(T) \tag{17}$$

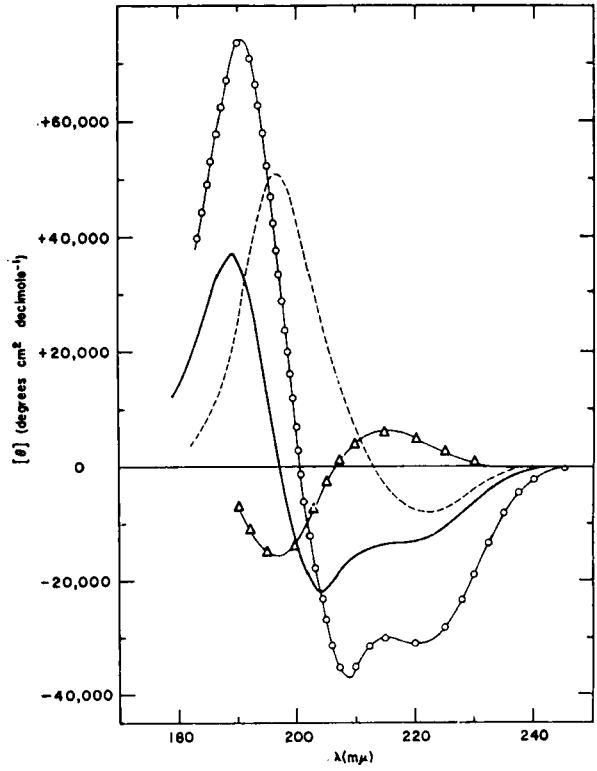

FIGURE 20(c) Circular dichroism spectra of different polypeptide conformations. The α-helix circular dichroism spectrum (○) is for poly(γ-methyl-L-glutamate) in hexafluoroisopropanol. The random chain spectrum (△) is for poly(γ-morpholinylethyl-L-glutamamide) in hexafluoroisopropanol. The β-structure spectrum (— — — —) is for poly(L-serine) in trifluoroethanol-water mixture (3:1).[2] (————) Poly(L-alanine) in hexafluoroisopropanol. Reprinted from Ref. (97) by courtesy of John Wiley & Sons, Inc.

$$\Delta H = RT_1T_2(T_2 - T_1)^{-1} \ln [x(T_2)/x(T_1)] \tag{18}$$

$$\Delta S = (\Delta H - \Delta G)/T \tag{19}$$

where $x(T)$ is the solubility of base expressed in units of mole fraction. Van't Hoff plots of log x vs. $1/T$ were always found to be linear, justifying the use of Eq. (18), which assumes the ΔH is temperature-independent over the range in question. Thermodynamic parameters of solution for nucleic acid bases are shown in Table XII. Thermodynamic parameters for transfer between two solvents were calculated from Table XII and are shown in Table XIII.

The most striking feature of the data in Tables XII and XIII is that exposure of any base to water from either initial state—crystal or organic solvent—

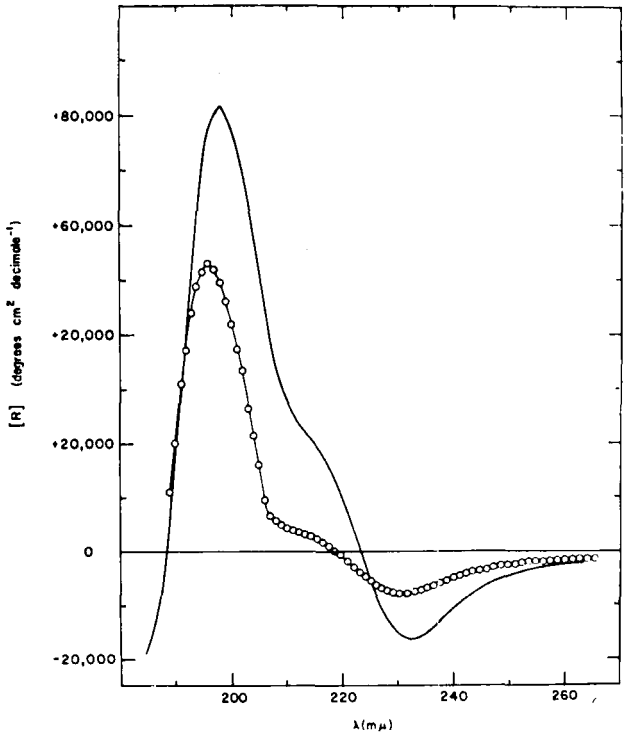

FIGURE 20(d) Optical rotatory dispersion of poly(L-alanine) in hexafluoroisopropanol (○) and in 1.06:3.00 water-hexafluoroisopropanol mixture (————). Reprinted from Ref. (97) by courtesy of John Wiley & Sons, Inc.

TABLE XII

Thermodynamic parameters of solution of nucleic acid bases at 37°C

	ΔF_{sol}(cal/mol)	ΔH_{sol} (cal/mol)	ΔS_{sol} (cal/deg mol)
Water			
Adenine	5170	7070	6.1
Cytosine	3750	7670	12.7
Uracil	4430	6700	7.3
CH_3OH			
Adenine	4660	3960	−2.3
Cytosine	4050	4220	0.6
Uracil	4590	6370	5.8
$CHCl_3$			
Adenine	8690	5590	−10.0

TABLE XIII

Thermodynamic parameters of transfer of bases from organic solvent to water at 37°C

Solvent	ΔF_{tr} (cal/mol)	ΔH_{tr} (cal/mol)	ΔS_{tr} (cal/deg mol)
From CH_3OH			
Adenine	510	2610	8.4
Cytosine	−300	3460	12.1
Uracil	−155	340	1.6
From $CHCl_3$			
Adenine	−3510	1480	16.1

results in positive values for ΔH and for ΔS. This corresponds to a net disruption of attractive interactions and a net disordering upon transfer of the base into water.

One might expect transfer from the crystal into water to involve large positive contributions to ΔH and ΔS from disruption of the crystal structure. Transfer from methanol or chloroform into water does not present this complication because crystal effects are removed from consideration. In fact, values of ΔH are markedly greater for transfer from the crystal to either an organic solvent or water than for transfer from organic solvent into water, most likely reflecting intermolecular forces in the crystal.

The values of ΔS for transfer into water in most cases fall in the range +5 to +12 entropy units, regardless of the identity of the base or the initial reference state. Values of ΔH for transfer from methanol into water are generally in the range of 1 to 3 kcal/mol (Table XIII). Higher values of ΔS and ΔH were observed for adenine and cytosine than for uracil.

The non-specific association of purines and pyrimidines in aqueous solution, the stacking and clustering together of the base residues in the interior of the double helical polynucleotide structures, and the disruption of ordered nucleic acid structures by organic solvents have all been attributed to hydrophobic interactions between the nucleic acid bases and water.[106–108] These workers have used the term "hydrophobic interaction" in the usual sense, the implication being that the bases are sufficiently non-polar to produce local ordering in water. This phenomenon can be studied by measuring the entropy of transfer from an organic environment into water; hydrophobic interaction is characterized by an entropy increase for this transfer. For nucleic acid bases, Scruggs *et al.* observed that this process is characterized by an entropy increase. Thus they conclude that the overall interaction of nucleic acid bases with water cannot be hydrophobic.

The evidence for hydrophobic interactions has been reviewed most recently by Ts'o.[108] The self-association of purine and pyrimidine derivatives in water is characterized by substantial negative entropies of association.[109,110] The entropies of self-association were found to be different for different compounds.

In order to account for the variation in the measured entropies, Ts'o asserts the existence of "hidden" positive contributions to the entropy, presumably arising from hydrophobic interactions. This interpretation of the data is then cited as evidence for hydrophobic interactions.

As a further example suggestive of hydrophobic interactions between nucleic acid bases and water, Ts'o draws upon the results of Crothers and Ratner,[111] who studied the thermodynamics of complex formation between deoxyguanosine and actinomycin in methanol-water mixtures. They found that the negative entropies of association increase in magnitude upon adding methanol, and pointed out that this result is consistent with the usual view of hydrophobic interactions. In view of the possibility that these hydrophobic effects arise from the interaction of actinomycin with water, these data do not demonstrate hydrophobic interaction of deoxyguanosine with water. Finally, the well-known phenomenon of disruption of ordered polynucleotide structures by organic solvents, while consistent with hydrophobic interaction, does not constitute proof that these interactions exist.

Recently, Lowe and Schellman[112] have measured the temperature-dependent CD and ORD spectra of ApA in dioxane-water mixtures. The addition of organic solvent leads to a large decrease in ΔH and a smaller proportional decrease in ΔS for the non-cooperative stacking interaction. These results provide additional and independent evidence against hydrophobic interactions and are entirely consistent with Scruggs *et al.* conclusions drawn from solubility measurements.

Thus there appears to be a considerable controversy as to the existence of hydrophobic bonding in stabilizing nucleic acid bases in solution as well as nucleic acid residues in polynucleotide structures in solution. It appears that a classic concept in solution chemistry, namely the hydrophobic bond, is not satisfactory in explaining the molecular thermodynamics of solutions containing nucleic acid bases and residues.

Herskovits and Harrington[113] have determined the solubilities of some of the nucleic acid bases and related nucleosides (adenine, adenosine, deoxyadenosine, thymine, guanosine, cytosine, and uracil) in water and various alcohol-water, ethylene glycol- and propylene glycol-water mixtures. Setschenow constants and related free energies of transfer of these bases and nucleosides from water to the various alcohol and glycol solutions have been determined. In general the increase in chain length or hydrocarbon content of the alcohols is found to increase the initial solubility of these compounds, giving increasingly more negative Setschenow constants and transfer free energies. Table XIV lists the thermodynamic quantities for the transfer of adenine and thymine from water to alcohol and ethylene glycol solutions at 35°C. Comparison of Table XIV and Table XII suggests the Herskovits and Harrington data are consistent with that of Scruggs *et al.* except for entropies.

TABLE XIV

Approximate thermodynamic functions of solution and transfer of adenine and thymine from water to alcohol and ethylene glycol solutions at 35°C

	Adenine			Thymine		
Solvent	ΔF°_{sol} kcal/mol	ΔH°_{sol} kcal/mol	ΔS°_{sol} cal/mol	ΔF°_{sol} kcal/mol	ΔH°_{sol} kcal/mol	ΔS°_{sol} cal/mol deg
Water	5.20	8.1	9.4	4.40	6.7	7.5
3 *M* Ethanol	4.73	8.1	10.9	4.17	6.5	7.6
6 *M* Ethanol	4.25	7.0	8.9	3.94	6.1	7.0
3 *M* l-Propanol	4.27	7.0	8.9	3.92	6.8	9.4
6 *M* l-Propanol	3.89	5.8	6.2	3.69	6.8	10.1
3 *M* Ethylene glycol	4.81	7.1	7.4	4.29	6.1	5.9
6 *M* Ethylene glycol	4.54	6.8	7.3	4.17	6.1	6.3
	ΔF_{tr} kcal/mol	ΔH_{tr} kcal/mol	ΔS_{tr} cal/mol deg	ΔF_{tr} kcal/mol	ΔH_{tr} kcal/mol	ΔS_{tr} cal/mol deg
6 *M* Ethanol	−0.95	−1.1	−0.5	−0.47	−0.6	−0.5
6 *M* l-Propanol	−1.3	−2.3	−3.2	−0.72	+0.1	+2.6
6 *M* Ethylene glycol	−0.66	−1.3	−2.1	−0.23	−0.6	−1.2

Reprinted from Ref. (113) by courtesy of the American Chemical Society.

This author is not able to resolve the entropy discrepancy. In comparison to the alcohols, the glycols appear to give less negative constants. Qualitatively, a close correlation is found between the solubility parameters and the effectiveness of the alcohols and glycols as DNA denaturants. The equations of Peller and Flory[114] which have been used to account for the effects of denaturants and salts on the denaturation transition and destabilization of proteins and polypeptides were extended to DNA denaturation, using the present Setschenow parameters corrected for self-interactions. The latter parameters and the binding constants calculated for the nonpolar portion of the alcohols, assuming a hydrophobic mechanism of alcohol-biopolymer interactions used in previous studies on proteins[115-117] were found to predict satisfactorily the various alcohol and glycol denaturation midpoints of T4 bacteriophage DNA at 73°, obtained by Levine *et al.*[118] Table XV presents the correlations observed between various properties of the alcohols and glycols as related to their capacity to denature DNA and proteins.

Another area of polymer solution chemistry which is receiving increasing attention is the phenomenon of chain aggregation in solution. Recently Matsumoto, Watanabe and Yoshioka[119] have studied the aggregation of poly(L-glutamic acid) (PGA) in aqueous methanol using electric birefringence. They found that the rise and decay of electric birefringence for PGA in aqueous solutions containing 20 and 10 vol % methanol are unusual. The decay curves

TABLE XV

Correlation between various properties of the alcohols and glycols related to their effectiveness as DNA and protein denaturants[a]

Alcohol or glycol	Molar refraction[b] cm^3	ΔF_{tr} of alkyl side chain of alcohol[c]	Distribution coefficient in olive oil-H_2O system	Denaturation midpoints of T4 phage DNA at 73°	ΔF_{tr} of average T4 phage DNA base at 25°[d] cal/mol	Denaturation midpoint of α-chymo-trypsinogen at 25°	ΔF_{tr} of indole at 25°[d] cal/mol
Methanol	8.2	−610	780	3.5 M	−19	7.2 M	−103
Ethanol	12.9	−1180	3200	1.2	−63	3.8	−151
1-Propanol	17.8	−1750	13,000	0.54	−170	1.6	−232
2-Propanol	17.6	−1450		0.90	−124	2.6	−186
1-Butanol	22.2	−2320		0.33	−311	0.7	−302
2-Butanol	22.1	−2020	25,000	0.62	−240	1.1	−240
tert-Butyl alcohol	22.2	−1720		0.60	−155	2.0	−195
Ethylene glycol	14.5	−610	49	2.2	−46	11.0	−108
Propylene glycol	18.1	−1180	170		−80	8.5	−160

[a]A breakdown as to how the data in this table has been assembled, including references, can be found in Levine *et al.*[118]

[b]Molar refraction, R, defined as $(M/d_T)\,(n_D^2-1)/(n_D^2+2)$, where M is the molecular weight, d_T is the density of the pure alcohol or glycol at temperature T (at 20° or 25°), and n_D is the refractive index at the sodium D line measured at the same temperature. The n_D and d_T values weretaken from the Handbook of Chemistry and Physics.

[c]Estimated values based on the free energies of transfer of amino acid side chains from water into 95% or 100% ethanol (Herskovits *et al.*[115]).

[d]Free energies of transfer of the average T4 bacteriophage DNA base and indole from water to 1.0 M alcohol and glycol solutions.

Reprinted from Ref. (113) by courtesy of the American Chemical Society.

were analyzed on the assumption that there exist two kinds of particles, namely, component I with a shorter relaxation time exhibiting positive birefringence and the other, component II, with a longer relaxation time exhibiting negative birefringence at low fields. Figure 21 shows the field strength dependence of the steady-state birefringence of both component I and

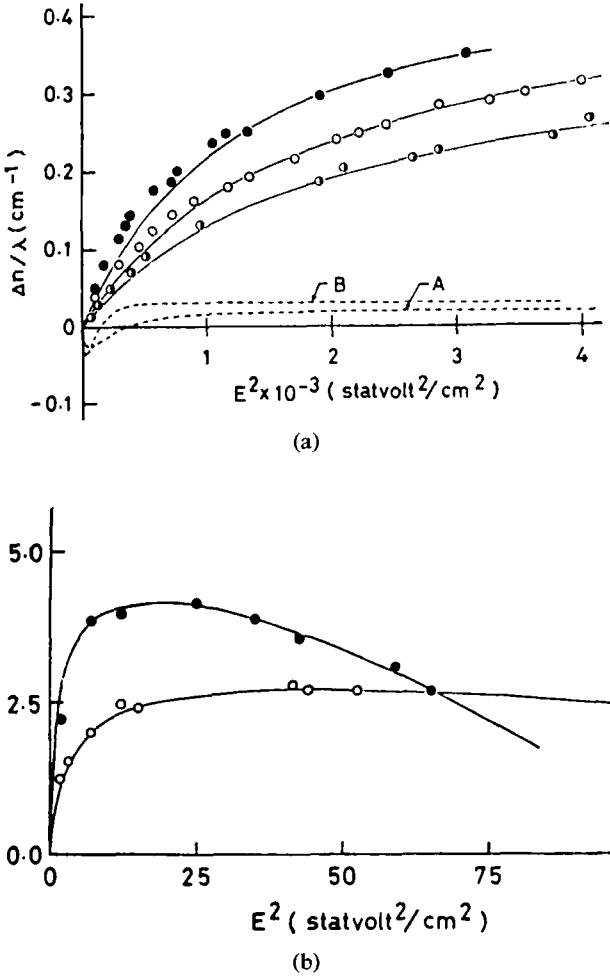

FIGURE 21 (*a*) Field strength dependence of the steady-state birefringence of PGA component I: (●) 30 vol % methanol; (○) 20 vol % methanol; (◑) 10 vol % methanol. Dashed curves are theoretical curves for component II: (A) 20 vol % methanol; (B) 10 vol % methanol. (*b*) Field strength dependence of the steady-state birefringence of PGA component II: (○) 20 vol % methanol; (●) 10 vol % methanol. Reprinted from Ref. (119) by courtesy of John Wiley & Sons, Inc.

component II. The drastic differences are obvious. From the field strength dependence of the steady-state birefringence the permanent dipole moment, the anisotropy of electric polarizability, and the saturation value of birefringence were determined for each component. Furthermore, from the relaxation time the length of component I and the diameter of component II were computed using the models of a cylindrical rod and an oblate ellipsoid, respectively. The dipole moment, the anisotropy of electric polarizability, and the relaxation time of component II are much larger than those of component I. Both the anisotropy of electric polarizability and the optical anisotropy factor are positive in sign for component I and negative for component II. It is concluded by the authors that component I is an isolated helical PGA molecule and component II is a side-by-side (anti-parallel) aggregate composed of many helical PGA molecules.

It is well known that the cationic acridine dyes are able to form stable complexes with DNA and a great number of publications investigate the structure and the properties of the complexes (see reviews, Refs. 120–123). After the fundamental work of Peacocke and Skerrett[124] in 1956 it seems very likely that the dye binding occurs in two processes: Process I corresponds to the monomer binding which includes interaction with the DNA bases; process II corresponds to an outside dye binding without any base specificity. The dye bound by process II can form longer polymeric units.

In order to obtain information on the binding forces involved in the formation of the complex proflavine-DNA by the stronger process I, the stability of the complexes was investigated by Lober, Schutz and Kleinwachter[125] in the presence of various organic solvents, methanol, ethanol, *n*-propanol, isopropanol, formamide, dimethyl sulfoxide, *p*-dioxane, glycerol, and ethylene glycol. Quantitative data on binding were obtained by means of absorption and fluorescence spectra, as well as by a thermal denaturation technique.

Lober *et al.* found that all organic solvents used decreased the binding ability of the dye. The effectiveness of the solvents increased with their hydrocarbon content, but could not be related to their dielectric constant. The complex formation was effectively suppressed by organic solvent concentrations, in which DNA still preserves its double-helical conformation. These results support the belief that hydrophobic forces are important in the formation of the complex proflavine-DNA in aqueous solution.

The similarity in spectroscopic properties of proflavine bound to DNA by process I and the same dye dissolved in an organic solvent made it possible to interpret the observed red shift of the long-wavelength absorption peak as being due to the interaction of the dye molecules with the less polar environment.

The same behavior was found for other dyes capable of intercalation like purified trypaflavine, phenosafranine and ethidium bromide. However,

Lober *et al.* concluded that intercalation is not a necessary condition, since they were able to show in the case of pinacyanol that it binds only at the surface of DNA.

The last studies presented here concerning solvation related phenomena deal with the solution conformations of peptide antibiotics. This writer feels that NMR studies of such systems have the potential to yield the most explicit estimation of the geometry accompanying the interaction of peptides with solvent. The small size and relatively fixed conformational states of many peptide oligomers combine to make precise local structural NMR probes possible.

Pitner and Urry[126] have carried out 220 MHz PMR studies of the antifungal tetradecapeptide antibiotic stendomycin in trifluoroethanol and methanol. Using three techniques, deuteron proton-exchange rates, chemical shift temperature dependence, and trifluoroethanol-solvent mixtures they concluded that all peptide protons were shielded, to varying degrees, from the solvent. These findings are in agreement with the work of Bodansky and Bodansky[127] who found that stendomycin did not react with the modified Rydon reagent, suggesting all peptide protons were "inside" the molecule. Pitner and Urry propose a folding of the lactone ring using β and β-like turns, and a left-handed α-helical segment for the series of D-amino acids in the linear segment.

Valinomycin is a cyclic dodecadepsipeptide having the sequence

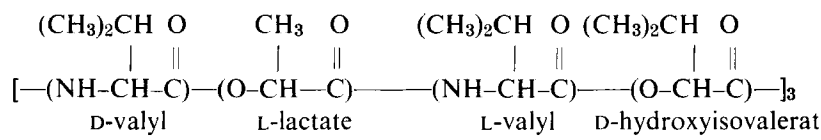

The conformation of valinomycin has been studied in solution by a variety of methods and also in the crystalline state. Ivanov *et al.*[128] examined the molecule in solution by infrared, optical rotatory dispersion, and dipole moment measurements, and these workers, as well as Haynes *et al.*,[129] Ohnishi and Urry,[130] and Urry and Ohnishi,[131] utilized nuclear magnetic resonance for conformational studies. In addition, Pinkerton *et al.*[132] presented a preliminary report of the crystal structure of the K^+ complex, while more recently Duax *et al.*[133] reported the crystal structure of valinomycin as crystallized from a nonpolar solvent, isooctane. The results of these studies may be summarized as follows.

In the K^+ complex the molecule has the shape of a bracelet, with the six amide NH groups intramolecularly hydrogen-bonded to the preceding amide carbonyls to form ten-membered rings. All six ester carbonyls point inward to give six-fold coordination about the unhydrated potassium ion. We will refer to this conformer as form *C*. The valyl HC^{α}-NH hydrogens are all *gauche*. Concerning the isopropyl side chains, the spin coupling constants indicate the HC^{α}-$C^{\beta}H$ protons are *trans* in the valyl residues and *gauche* in the hydroxy-

isovaleryl residues. This molecular conformation is compatible with the result of the partial crystal-structure analysis reported for the potassium aurichloride complex by Pinkerton *et al.*[132] Furthermore, the structure of the complex appears to be quite rigid, as evidenced by the observation that changes in the solvent polarity from ethanol to 3:1 heptane-ethanol do not affect the shape of the ORD curve (Ivanov *et al.*[128]) and that the α-proton chemical shifts are nearly independent of temperature (Ohnishi and Urry[130,131]). Haynes *et al.*[129] showed that the NMR spectrum of the carefully dried complex in $CDCl_3$ was unaffected by the addition of 2 μl of H_2O per ml of solution.

The situation is more complicated for valinomycin containing no complexed cation. The preferred conformation in nonpolar solvents (which we will designate as form *A*) resembles the K^+ complex in having all six amide NH groups hydrogen-bonded intramolecularly. However, the crystal structure (Duax *et al.*[133]) indicates a different intramolecular hydrogen bonding scheme, with two of the six forming 13-membered rings. Also, two of the ester carbonyls are found to point toward the center, while four are directed outward (two parallel to the axis of the bracelet and two perpendicular to this axis). These features are not in agreement with the deductions based upon solution studies but, as Duax *et al.*[133] have pointed out, this conformation is compatible with the observations of solution studies. Coupling constant measurements indicate the HN-C^{α}H protons are again *gauche* for the L-valyl residues, but are *cis* for the D-valyl residues. The isopropyl HC^{α}-C^{β}H protons are *trans* in the valyl residues and *gauche* in the hydroxyisovaleryl residues, as was the case for the *C* form.

The ORD, IR, NMR data and the temperature dependence of the chemical shifts all indicate that the *A* form of valinomycin is in dynamic equilibrium with a second conformer, which we will refer to as form *B*, and that the latter is favored in more polar solvents such as methanol and dimethyl sulfoxide. This form has only the three D-valyl NH groups intramolecularly hydrogen bonded, and all six HN-C^{α}H protons are *cis*. The isopropyl groups of the valyl residues are more nearly freely rotating in form *B*. The ORD curves (Ivanov *et al.*)[129] give clear evidence of the equilibrium between the *A* and *B* forms. Ohnishi and Urry[130] found that although only one type of valyl NH is hydrogen bonded intramolecularly, both exchange with deuterium at nearly the same rate in dimethyl sulfoxide solution. Hence, these authors propose two dish-shaped *B* conformers having nearly the same energy, and interconverting via the *A* form.

6 SUMMARY

This paper has attempted to review the status of our understanding of the interaction of macromolecules with solvent molecules and the degree to which

each induces order in the other. Historically, the first attempt to describe polymer solutions were based upon chain-lattice models and the thermodynamic properties of the solutions were of principal interest. Recent studies of the solvated state of polymers focus upon the detailed molecular interactions between solute and solvent species. The bulk of this work has been carried out for biopolymers, especially the polypeptides. Modern experiments in polymer solution studies dwell upon the inter-relationship between the dynamics of chain conformation in the polymer and the ordering of solvent molecules about the chain. Perhaps it is an overly optimistic statement, but it appears, both experimentally and theoretically, that we are poised in a position to make major breakthroughs in our understanding of the solvated state.

References

1. P. J. Flory, *J. Chem. Phys.* **10,** 51 (1942).
2. M. L. Huggins, *Ann. N.Y. Acad. Sci.* **43,** 1 (1942); *J. Phys. Chem.* **46,** 151 (1942; *J. Amer. Chem. Soc.* **64,** 1712 (1942).
3. G. Gee and W. J. C. Orr, *Trans. Faraday Soc.* **42,** 507 (1946).
4. P. J. Flory and W. R. Krigbaum, *J. Chem. Phys.* **18,** 1086 (1950).
5. I. Prigogine, *The Molecular Theory of Solutions* (Interscience, New York, 1957).
6. P. J. Flory, J. L. Ellenson, and B. E. Eichinger, *Macromolecules* **1,** 279 (1968).
7. B. E. Eichinger and P. J. Flory, *Trans Faraday Soc.* **64,** 2035 (1968).
8. B. E. Eichinger and P. J. Flory, *Trans Faraday Soc.* **64,** 2053 (1968).
9. B. E. Eichinger and P. J. Flory, *Trans Faraday Soc.* **64,** 2061 (1968).
10. B. E. Eichinger and P. J. Flory, *Trans Faraday Soc.* **64,** 2066 (1968).
11. D. Patterson, *Rubber Chem. Tech.* **40,** 1 (1967).
12. D. Patterson, *Macromolecules* **2,** 672 (1969).
13. S. H. Maron, *J. Polymer Sci.* **38,** 329 (1959).
14. S. H. Maron and C. A. Daniels, *J. Macromol. Sci.* **B2,** 743 (1968).
15. S. H. Maron and Min-Shiu Lee, *J. Macromol. Sci.* **B7,** 61 (1973).
16. A. D. McLaren and J. W. Rowen, *J. Polymer Sci.* **1,** 289 (1951).
17. L. Valentine, *Ann. Sci. Text. Belg.* **4,** 206 (1955).
18. D. D. Eley and R. B. Leslie, *Advan. Chem. Phys.* **1,** 238 (1964).
19. H. J. C. Berendsen, Biological Significance of Water Structure, in *Biology of the Mouth,* (American Association for Advancement of Science, 1968) pp. 145–167.
20. R. L D'Arcy and I. W. Watt, *Trans. Faraday Soc.* **66,** 1230 (1970).
21. I. C. Watt and J. D. Leeder, *J. Text. Inst.* **59,** 353 (1968).
22. M. M. Breuer and M. G. Kennerley, *J. Colloid Interfac. Sci.* **37,** 124 (1971).
23. Y. N. Chirgadze and A. M. Ovsepyan, *Biopolymers* **11,** 2179 (1972).
24. E. R. Blout and H. Lenormant, *Nature* **179,** 960 (1957); H. Lenormant, A. Baudras, and E. R. Blout, *J. Amer. Chem. Soc.* **80,** 6191 (1958).
25. U. Shmueli and W. Traub, *J. Mol. Biol.* **12,** 205 (1965).
26. V. V. Kobyakov, in *Properties and Functions of Macromolecules and Macromolecular Systems* (in Russian) (Nauka, Moscow, 1969), p. 42.
27. W. C. McCabe and H. F. Fisher, *Nature* **207,** 1274 (1965).
28. W. C. McCabe and H. F. Fisher, *J. Phys. Chem.* **74,** 2990 (1970).
29. S. Subramanian and H. F. Fisher, *Biopolymers* **11,** 1305 (1972).
30. H. Noguchi and J. T. Yang, *Biopolymers* **1,** 359 (1963).
31. H. Noguchi, *Biopolymers* **4,** 1105 (1966).
32. H. A. Scheraga, *Protein Structure* (Academic Press, New York, 1961), Chapter VI.

33. E. J. Cohn and J. T. Edsall, *Proteins, Amino Acids and Peptides* (Reinhold, New York, 1943), p. 16.
34. D. P. Stevenson, in *Structural Chemistry and Molecular Biology*, edited by A. Rich and N. R. Davidson (W. H. Freeman and Co., San Francisco, Calif., 1968), p. 490.
35. S. Hanlon, in *Spectroscopic Approaches to Biomolecular Conformation*, edited by D. W. Urry, (American Medical Association, Chicago, Ill., 1970), Chapter V.
36. P. Doty and W. Gratzer, in *Polyamino Acids, Polypeptides and Proteins*, edited by M. A. Stahmann (University of Wisconsin Press, Madison, Wisc., 1962), p.111.
37. U. Buontempo, G. Careri, and P. Fasella, *Biopolymers* **11,** 519 (1972).
38. E. G. Bendit, *Biopolymers* **4,** 539 (1966).
39. C. G. Cannon, B. C. Stace, and R. Jeffries, *Nature* **196** (1962).
40. H. Strassmair, J. Engel, and G. Zundel, *Biopolymers* **8,** 237 (1969).
41. H. Strassmair, J. Engel and S. Knof, *Biopolymers*, in press.
42. S. Knof, H. Strassmair, J. Engel, M. Rothe, and K. D. Steffen, *Biopolymers* **11,** 731 (1972).
43. C. M. Venkatachalam, *Biochim. Biophys. Acta* **168,** 397 (1968).
44. IUPAC–IUB Commission on Biochemical Nomenclature, "Abbreviations and Symbols for the Description of the Conformation of Polypeptide Chains. Tentative Rules (1969)", *Biochemistry* **9,** 3471 (1970).
45. M. Rothe, R. Theysohn, K. D. Steffen, M. Kostrzewa, and M. Zamani, *Peptides*, Proc. 10th European Peptide Symposium, Abano Terme, 1969, p. 179.
46. V. Ganser, J. Engel, D. Winklmair, and G. Kruse, *Biopolymers* **9,** 329 (1970).
47. C. A. Swenson and R. Formanek, *J. Phys. Chem.* **71,** 4073 (1967).
48. M. E. Fuller and W. S. Brey, *J. Biol. Chem.* **243,** 274 (1968).
49. I. D. Kuntz, T. S. Bassfield, G. D. Law, and P. V. Purcell, *Science* **163,** 1329 (1969).
50. H. J. C. Berendsen, *J. Chem. Phys.* **36,** 3297 (1962).
51. J. A. Glasel, *J. Amer. Chem. Soc.* **92,** 375 (1970).
52. G. Nemethy and H. A. Scheraga, *J. Chem. Phys.* **36,** 3401 (1962).
53. K. D. Gibson and H. A. Scheraga, *Proc. Nat. Acad. Sci. U.S.* **58,** 420 (1967).
54. F. R. Brown III, A. J. Hopfinger, and E. R. Blout, *J. Mol. Biol.* **63,** 101 (1972).
55. A. Yonath and W. Traub, *J. Mol. Biol.* **43,** 461 (1969).
56. F. R. Brown, A. di Corato, A. Lorenzi, and E. R. Blout, *J. Mol. Biol.* **63,** 85 (1973).
57. Y. Kobayashi, R. Sakai, K. Kakiuchi, and T. Isemura, *Biopolymers* **9,** 415 (1970).
58. D. M. Segal, *J. Mol. Biol.* **43,** 497 (1969).
59. S. Krimm and C. M. Venkatachalam, *Proc. Nat. Acad. Sci. U.S.* **68,** 2468 (1971).
60. L. Mandelkern, in *Poly-α-Amino Acids*, edited by G. D. Fasman (Marcel Dekker, New York, 1967), p. 675.
61. E. A. Moelwyn-Hughes, *Physical Chemistry* (Pergamon Press, New York, 1957).
62. W. C. Davidon, AEC Research and Development Report No. ANL-5090, 1959.
63. A. J. Hopfinger, *Conformational Properties of Macromolecules* (Academic Press, New York, 1973).
64. A. Bondi, *J. Phys. Chem.* **68,** 441 (1964).
65. A. J. Hopfinger, *Macromolecules* **4,** 731 (1971).
66. D. Aebersold and E. S. Pysh, *J. Chem. Phys.* **53,** 2156 (1970).
67. F. K. Winkler and J. D. Dunitz, *J. Mol. Biol.* **59,** 169 (1971).
68. D. A. Brant, W. G. Miller, and P. J. Flory, *J. Mol. Biol.* **23,** 47 (1967).
69. A. J. Hopfinger, *Ph.D. Thesis*, Case Western Reserve University, Cleveland, Ohio, 1969.
70. T. Ooi, R. A. Scott, G. Vanderkooi ,and H. A. Scheraga, *J. Chem. Phys.* **46,** 4410 (1967).
71. J. A. Schellman, *C. R. Trav. Lab. Carlsberg, Ser. Chim.* **29,** 223, 230 (1955).
72. S. Krimm and J. Mark, *Proc. Nat. Acad. Sci. U.S.* **60,** 1122 (1968).
73. D. Balasubramanian, *Chem. Commun.*, 862 (1970).
74. A. J. Adler, R. Hoving, J. Potter, M. Wells, and G. D. Fasman, *J, Amer. Chem. Soc.* **90,** 4736 (1968).
75. G. D. Fasman, private communication.
76. J. Steigman, E. Peggion, and A. Cosani, *J. Amer. Chem. Soc.* **91,** 1822 (1969).
77. E. Peggion, L. Strasorier, and A. Cosani, *J. Amer. Chem. Soc.* **92,** 381 (1970).

78. V. Sasisekharan, *Acta Crystallogr.* **12,** 897 (1959).
79. Examples of this conformation in proline residues are found for pro 68 and pro 168 of papian, pro 70 of lysozyme, and pro 94, pro 214 and pro 288 of carboxy peptidase A.
80. H. Okabayashi, T. Isemura, and S. Sakakibava, *Biopolymers* **6,** 323 (1968).
81. W. Traub and V. Shmueli, *Nature* **198,** 1165 (1963).
82. H. W. Wyckoff, D. Tsernoglou, A. W. Hanson, J. R. Knox, B. Lee, and F. M. Richards, *J. Biol. Chem.* **245,** 305 (1970).
83. C. K. Johnson, ORTEP II, Report N. ORNL-3794, Oak Ridge National Laboratory, Oak Ridge, Tennessee.
84. a) W. A. Klee, *Biochemistry* **7,** 2731 (1968).
b) J. E. Brown and W. A. Klee, *Biochemistry* **10,** 470 (1971).
85. H. Brumberger and L. C. Anderson, *Biopolymers* **11,** 679 (1972).
86. L. C. Anderson, *Ph.D. Thesis*, Syracuse University, Syracuse, N.Y., 1968.
87. L. C. Anderson, H. Brumberger, and R. H. Marchessault, *Nature* **216,** 52 (1967).
88. C. H. Bamford, A. Elliot, and W. E. Hanby, *Synthetic Polypeptides* (Academic Press, New York, 1956), Chapter 5.
89. H. D. Keith and F. J. Padden, *J. Appl. Phys.* **36,** 2987 (1965).
90. T. Miyazawa, in *Poly-α-Amino Acids*, edited by G. D. Fasman, (Marcel Dekker, New York, 1967), Chapter 2.
91. A. Nakajima and M. Murakami, *Biopolymers* **11,** 1295 (1972).
92. D. A. Brant and P. J. Flory, *J. Amer. Chem. Soc.* **87,** 2788 (1965).
93. K. Nagai, *J. Chem. Phys.* **34,** 887 (1961).
94. W. G. Miller and P. J. Flory, *J. Mol. Biol.* **15,** 298 (1966).
95. M. Go, N. Saito, and M. Ochiai, *J. Phys. Soc. Japan* **22,** 227 (1967).
96. A. Teramoto, T. Norisuye, and H. Fujita, *Polymer J.* **1,** 55 (1970).
97. J. R. Parrish, Jr. and E. R. Blout, *Biopolymers* **11,** 1001 (1972).
98. J. R. Parrish, Jr. and E. R. Blout, *Biopolymers* **10,** 1491 (1971).
99. F. Quadrifoglio and D. W. Urry, *J. Amer. Chem. Soc.* **90,** 2760 (1968).
100. T. Miyazawa and E. R. Blout, *J. Amer. Chem. Soc.* **83,** 712 (1961).
101. P. K. Sarkar and P. Doty, *Proc. Nat. Acad. Sci. U.S.* **55,** 981 (1966).
102. E. Iizuka and J. T. Yang, *Proc. Nat. Acad. Sci. U.S.* **55,** 1175 (1966).
103. R. Townsend, T. F. Kumosinski, and S. N. Timasheff, *Biochem. Biophys. Res. Comm.* **23,** 163 (1966).
104. N. Greenfield and G. D. Fasman, *Biochemistry* **10,** 4108 (1969).
105. R. L. Scruggs, E. K. Achter, and P. D. Ross, *Biopolymers* **11,** 1961 (1972).
106. D. M. Crothers and B. H. Zimm, *J. Mol. Biol.* **9,** 1 (1964).
107. T. T. Herskovits, S. J. Singer, and E. P. Geiduschek, *Arch. Biochem. Biophys.* **94,** 99 (1961).
108. P. O. P. Ts' o, in *Fine Structure of Protein and Nucleic Acids*, edited by G. D. Fasman and S. N. Timasheff (Marcel Dekker, New York, 1970), Chapter 2, pp.166–168.
109. S. J. Gill, M. Downing, and G. F. Sheats, *Biochemistry* **6,** 272 (1967).
110. E. L. Farquhar, M. Downing, and S. J. Gill, *Biochemistry* **7,** 1224 (1968).
111. D. M. Crothers and D. I. Ratner, *Biochemistry* **7,** 1827 (1968).
112. M. J. Lowe and J. A. Schellman, *J. Mol. Biol.* **65,** 91 (1972).
113. T. T. Herskovits and J. P. Harrington, *Biochemistry* **11,** 4800 (1972).
114. L. Peller, *J. Phys. Chem.* **63,** 1199 (1959).
115. T. T. Herskovits, B. Gadegbeku, and H. Jaillet, *J. Biol. Chem.* **245,** 2588 (1970).
116. T. T. Herskovits, H. Jaillet, and A. T. DeSena, *J. Biol. Chem.* **245,** 6511 (1970).
117. T. T. Herskovits, H. Jaillet, and B. Gadegbeku, *J. Biol. Chem.* **245,** 4544 (1970).
118. L. Levine, J. A. Gordon, and W. P. Jencks, *Biochemistry* **2,** 168 (1963).
119. M. Matsumoto, H. Watanabe, and K. Yoshioka, *Biopolymers* **11,** 1711 (1972).
120. A. Blake and A. R. Peacocke, *Biopolymers* **6,** 1225 (1968).
121. D. O. Jordon, *Molecular Associations* (Academic Press, New York, 1968) p. 221.
122. G. Lober, *Z. Phys. Chem.* (*Frankfurt am Main*) **9,** 252 (1969).
123. G. Lober, *ibid.* **11,** 92, 135 (1971).
124. A. R. Peacocke and J. N. H. Skerrett, *Trans. Faraday Soc.* **52,** 216 (1956).

125. G. Lober, H. Schutz, and V. Kleinwachter, *Biopolymers* **11,** 2439 (1972).
126. T. P. Pitner and D. W. Urry, *Biochemistry* **11,** 4132 (1972).
127. M. Bodansky and A. Bodansky, *Nature* **220,** 73 (1968).
128. V. T. Ivanov, I. A. Laine, N. D. Abdulaev, L. B. Senyavina, E. M. Popov, Y. A. Ovchinnikov, and M. M. Shemyskin, *Biochem. Biophys. Res. Comm.* **34,** 803 (1968).
129. D. H. Hayes, A. Kowalsky, and B. C. Pressman, *J. Biol. Chem* **244,** 502 (1969).
130. M. Ohnishi and D. W. Urry, *Biochem. Biophys. Res. Comm.* **36,** 194 (1969).
131. M. Ohnishi and D. W. Urry, *Science* **168,** 1091 (1970).
132. M. Pinkerton, L. K. Steinrauf, and P. Dawkins, *Biochem. Biophys. Res. Comm.* **35,** 512 (1969).
133. W. L. Duax, H. Hauptman, C. M. Weeks, and D. A. Norton, *Science* **176,** 911 (1972).
134. K. H. Forsythe and A. J. Hopfinger, *Macromolecules* **6,** 423 (1973).

DISCUSSION

Prof. S. Krause (*Rensselaer Polytechnic Institute, Troy, New York*): If you find no changes in the energies of the *cis* and *trans* poly(L-proline) helices with changes in solvent, what is the driving force for the formation of one or the other form in a particular solvent and what is the driving force for the transition from one form to the other?

Prof. A. Hopfinger: First, we do note slight differences in the solvent preference of the *cis* and *trans* forms. The *cis* form likes more hydrophobic solvents than the *trans* form. This is in agreement with experiment. Secondly, our model is too crude so as to be able to predict the consequences of pH, i.e., ionic content, of a solvent medium. Since it is ionic protonation which initiates the onset of *cis* $\rightleftarrows$ *trans* interconversion in poly(L-proline) our model cannot discern the origins of the transition driving force.

Prof. P. L. Luisi (*Swiss Federal Institute of Technology, Zurich*): You showed that for a series of polypeptides the calculated conformation depends upon the nature of the solvent. As far as the comparison with experimental data is concerned: is always the conformation you calculate in vacuum the one which is closer to the conformation found by X-rays in the crystalline state?

Prof. A. Hopfinger: There is no definite answer to this question since more than one type of crystal structure is usually possible for most homopolypeptide chains. I would say that our calculations suggest that the solution conformations calculated as being energy minima are the chain conformations found in the solid state for crystals formed from chains precipitated out of each of the respective solvents. That is, solution and solid state conformations are identical for a particular solvent medium and/or precipitate. Our sampling of cases where there is experimental evidence to substantiate the above conjecture is small and, hence, the general validity of our findings should be viewed with reserve.

Prof. L. Tiffany (*University of Michigan, Ann Arbor, Michigan*): Have you considered why poly(L-serine) is not water soluble while poly(L-proline) II is very water soluble? Have you tried to calculate the interaction of gem-diols with the polypeptide chains?

Prof. A. Hopfinger: We have not explicitly carried out solvent-dependent conformational studies of poly(L-serine). However, we would speculate that poly(L-serine) is not very water soluble because the locally ordered conformation is α-helical with the side-chain OH groups involved with the backbone NH groups in a bifurcated hydrogen bond with backbone carbonyl oxygens. In the case of poly(L-proline) both the *trans* and *cis* (but to a lesser extent) conformations project the C = O groups out into solvent. This promotes solvation. We have not attempted any solvation calculations using the hydration shell model for gem-diols and polypeptide chains.